*Molecules* **2015**, *20*, 8242-8269; doi:10.3390/molecules20058242

OPEN ACCESS

*molecules*

**ISSN 1420-3049**

www.mdpi.com/journal/molecules

*Article*

# Celastrol Protects against Antimycin A-Induced Insulin Resistance in Human Skeletal Muscle Cells

**Mohamad Hafizi Abu Bakar [1,*], Kian-Kai Cheng [1,2], Mohamad Roji Sarmidi [2,3,*], Harisun Yaakob [3] and Hasniza Zaman Huri [4,5]**

1 Department of Bioprocess Engineering, Faculty of Chemical Engineering, Universiti Teknologi Malaysia, 81310 Johor Bahru, Johor, Malaysia; E-Mail: chengkiankai@cheme.utm.my

2 Innovation Centre in Agritechnology for Advanced Bioprocessing (ICA), Universiti Teknologi Malaysia, 81310 Skudai, Johor, Malaysia

3 Institute of Bioproduct Development, Universiti Teknologi Malaysia, 81310 Johor Bahru, Johor, Malaysia; E-Mail: harisun@ibd.utm.my

4 Department of Pharmacy, Faculty of Medicine, University of Malaya, 50603 Kuala Lumpur, Malaysia; E-Mail: hasnizazh@ummc.edu.my

5 Clinical Investigation Centre, 13th Floor Main Tower, University Malaya Medical Centre, 59100 Lembah Pantai, Kuala Lumpur, Malaysia

* Authors to whom correspondence should be addressed; E-Mails: mhafizi55@live.utm.my (M.H.A.B.); mroji@ibd.utm.my (M.R.S.); Tel.: +601-3308-4071 (M.H.A.B.); Fax: +607-5569-706 (M.H.A.B.).

Academic Editor: Maurizio Battino

*Received: 30 March 2015 / Accepted: 4 May 2015 / Published: 7 May 2015*

---

**Abstract:** Mitochondrial dysfunction and inflammation are widely accepted as key hallmarks of obesity-induced skeletal muscle insulin resistance. The aim of the present study was to evaluate the functional roles of an anti-inflammatory compound, celastrol, in mitochondrial dysfunction and insulin resistance induced by antimycin A (AMA) in human skeletal muscle cells. We found that celastrol treatment improved insulin-stimulated glucose uptake activity of AMA-treated cells, apparently via PI3K/Akt pathways, with significant enhancement of mitochondrial activities. Furthermore, celastrol prevented increased levels of cellular oxidative damage where the production of several pro-inflammatory cytokines in cultures cells was greatly reduced. Celastrol significantly increased protein phosphorylation of insulin signaling cascades with amplified expression of AMPK protein and attenuated NF-κB and PKC $\theta$ activation in human skeletal muscle treated with AMA. The improvement

of insulin signaling pathways by celastrol was also accompanied by augmented GLUT4 protein expression. Taken together, these results suggest that celastrol may be advocated for use as a potential therapeutic molecule to protect against mitochondrial dysfunction-induced insulin resistance in human skeletal muscle cells.

**Keywords:** celastrol; mitochondrial dysfunction; inflammation; human skeletal muscle; nuclear factor kappa B

## 1. Introduction

Over the past few decades, the global prevalence and incidence rate of type 2 diabetes mellitus has been escalating world-wide. It is currently estimated that over 350 million people world-wide suffer from this disease, and this figure is projected to rise to 600 million in 2035 [1,2]. The exact mechanism underpinning type 2 diabetes is still unknown, but oxidative stress, inflammation and mitochondrial dysfunction have been suggested to be among the central events contributing to the development of the disorder [3,4]. This postulation is perpetuated by a wealth of experimental and epidemiological studies showing that the impairment of mitochondrial functions in the skeletal muscle, liver and adipose tissues of both human and animal models are orchestrated by aberrant insulin signaling activities [3,5–8].

To date, the precise link and interaction between mitochondrial dysfunction and insulin signaling pathways is still largely debated [3,9]. Substantial evidence from previous literature has pointed out that Complex I and III in the electron transport chain of mitochondria are major contributors to oxidative stress in diabetic patients [10,11]. Excessive accumulation of mitochondrial reactive oxygen species (ROS) production and chronic inflammation in peripheral tissues may lead to oxidative stress, thus leading to the oxidation of numerous intracellular components, including DNA, protein and membrane phospholipids. This process results in the activation of stress signaling pathways that participate in the development of insulin resistance. The activation of several oxidative stress-induced inflammation pathways, including c-Jun N-terminal kinases (JNK), protein kinase C (PKC), glycogen synthase kinase 3 (GSK-3), nuclear factor-κB (NF-κB), and p38 mitogen-activated protein kinases (MAPK), have been shown to synergistically impair insulin signaling pathways. Notably, mounting evidence has shown that the central event connecting these cellular perturbations is severe disturbance of mitochondrial functions [3,9].

Skeletal muscle is a major site of postprandial glucose disposal and the main target organ for various metabolic activities [12]. Elevated circulating free fatty acid-induced lipotoxicity and impairment of oxidative metabolism directly affect the insulin-stimulated glycogen synthesis in skeletal muscle [13]. High levels of intracellular C18:2 CoA, ceramides and diacylglycerols (DAGs) were associated with reduced mitochondrial functions and insulin signaling activity [3]. In this system, the defects in phosphorylation of tyrosine residue and amplified phosphorylation of serine residue in insulin receptor substrate-1 (IRS1) result in reduced IRS-1 associated PI3K activity with a concomitant increase of PKC $\theta$ activation [8]. The concerted action of these alterations in oxidative profiles of skeletal muscle leads to weakened insulin-stimulated glucose uptake via decreased glucose transporter-4 (GLUT4) translocation due to declined phosphorylation of AKT and its downstream effectors [14]. The defects in glucose

transport activity and diminished functions of phosphoinositide 3-kinase (PI3K) activity are among the direct consequences of cellular damage and oxidized biomolecules. Eventually, these perturbations lead to the activation of several inflammatory pathways including NF-κB and IκB kinase β (IKKβ) signaling and consequently enhance the expression of certain target genes responsible for interleukin-6 (IL-6), tumor necrosis factor-α (TNF-α) and interleukin-1β (IL-1β) production [15]. To a lesser extent, the chronic stimulation of these inflammatory pathways have been recognized as the "main culprits" that contribute to the progression of type 2 diabetes. Hence, further therapeutic interventions and prevention should be modulated towards targeting these regulatory pathways while boosting the metabolic pathways that promote enhanced cellular bioenergetics.

Celastrol is an active ingredient of natural quinine-methide triterpenoid isolated from the plant family *Celastraceae* (*Tripterygium wilfordii* Hook F.), the traditional Chinese medicine also known as "Thunder God Vine." This compound exhibits various biological activities including anti-oxidant, anti-inflammatory and anti-cancer properties [16]. In addition, celastrol was found able to inhibit NF-κB transcription factors and its downstream targets in various cell types without affecting the DNA-binding activity of activator protein 1 (AP-1) [17–19]. Recently, celastrol has shown to possess anti-diabetic effects on diabetic nephropathy and improve whole-body insulin resistance [20]. The authors observed that *in vivo* administration of celastrol for 2 months in six-week-old male diabetic *db/db* mice (C57BLKS/J-*lepr*$^{db}$/*lepr*$^{db}$) improved insulin resistance, oxidative stress and glycemic control with substantial restoration of renal functional and diabetes-induced structural changes. In other cell types, celastrol was shown to exhibit cytoprotective properties in vascular smooth muscle cells (VSMCs) and myocardioblast via heme oxygenase-1 (HO-1) induction [21,22]. However, the effects of celastrol on the amelioration of mitochondrial dysfunction-induced oxidative damage in skeletal muscle cells with insulin resistance are not currently available.

We have previously reported that celastrol improved the oxidative metabolism of adipocytes with mitochondrial dysfunction via inhibition of NF-κB signaling pathways [23]. On the basis of these observations, it is of interest to investigate the effects of celastrol on mitochondrial dysfunction and insulin resistance in human skeletal muscle-derived myoblast. In this context, the present study established an *in vitro* model of mitochondrial dysfunction and insulin resistance in human skeletal muscle induced by antimycin A (AMA), a mitochondrial Complex III inhibitor. The results showed that celastrol can protect the cells from AMA-induced insulin resistance and mitochondria dysfunction. This is achieved via significant improvement in glucose uptake activity, mitochondria functions and oxidative metabolism, enhanced insulin signaling cascade pathways, and its downstream effectors.

## 2. Results and Discussion

### *2.1. Effects of AMA and Celastrol Treatment on Cell Viability (Dose and Time-Dependent)*

Firstly, dose and time-dependent MTT assays were performed to determine the effect of AMA and celastrol on viability of skeletal muscle cells. After serum starvation, cells were treated with a series of concentrations (15, 30, 60, 120 μM and nM for both AMA and celastrol, respectively) for 24 h. As shown in Figure 1A,B, both AMA and celastrol reduced cell viability in a dose-dependent manner. The optimal concentration of AMA that did not significantly inhibit cell viability was 30 μM. The result also

showed that celastrol at the doses of 30, 60 and 120 nM significantly decreased cell viability by 35%, 46% and 49%, respectively. Therefore, celastrol at a dose of 15 nM was chosen for all subsequent experiments. Moreover, we also performed the time-dependent evaluation (12, 24, 36 and 48 h) for cells treated with the selected single concentrations of 30 μM AMA and 15 nM celastrol (Figure 1C). There was no significant effect on cell viability after AMA and celastrol treatment for 48 h. A number of studies reported that the optimal doses of celastrol that did not significantly inhibit cell viability were found to be in the nano-molar range, with an incubation time of no more than 24 h [22,24,25]. Furthermore, another group observed that continuous exposure of celastrol at sub-micromolar concentrations is linked to reduced cellular viability and proliferation [26]. Consistently, our result showed that an incubation of 15 nM celastrol in human skeletal muscle cells for 48 h did not affect cell viability.

As shown in Figure 1D, human skeletal muscle cell treated with low dose DMSO as control exhibits a typical epithelial phenotype with small polygonal shapes. Co-incubation with AMA treatment alone (Figure 1E) induces enlargement of cytoplasm with a tight arrangement linking the cells. However, when exposed to 15 nM celastrol in AMA-treated cells, cells acquired a spindle-shaped structure with variable sizes (Figure 1F). To avoid other confounding factors, cells were treated with celastrol only. As depicted in Figure 1G, celastrol treatment alone induces morphological changes in the cells that are somewhat similar to the treatment with celastrol on AMA-treated cells with multi-nucleated cells.

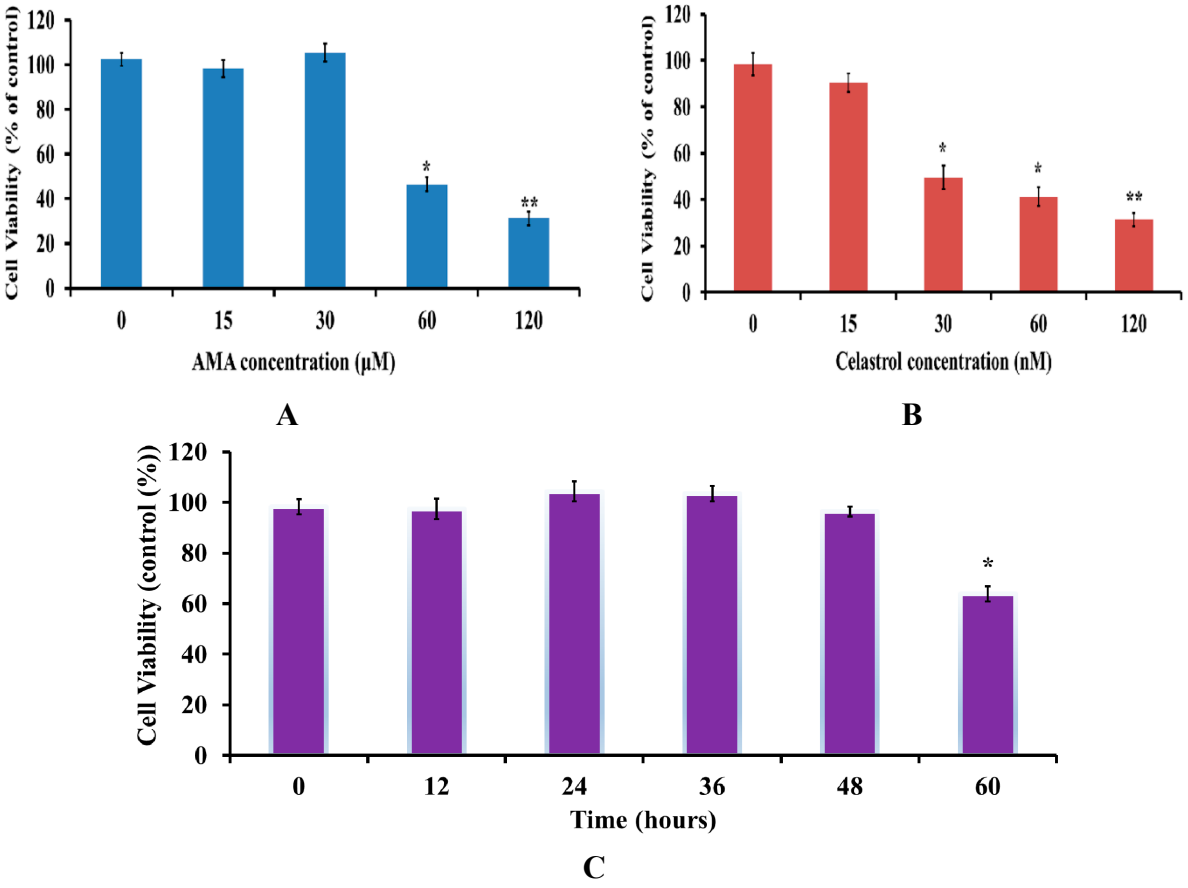


**Figure 1.** *Cont.*

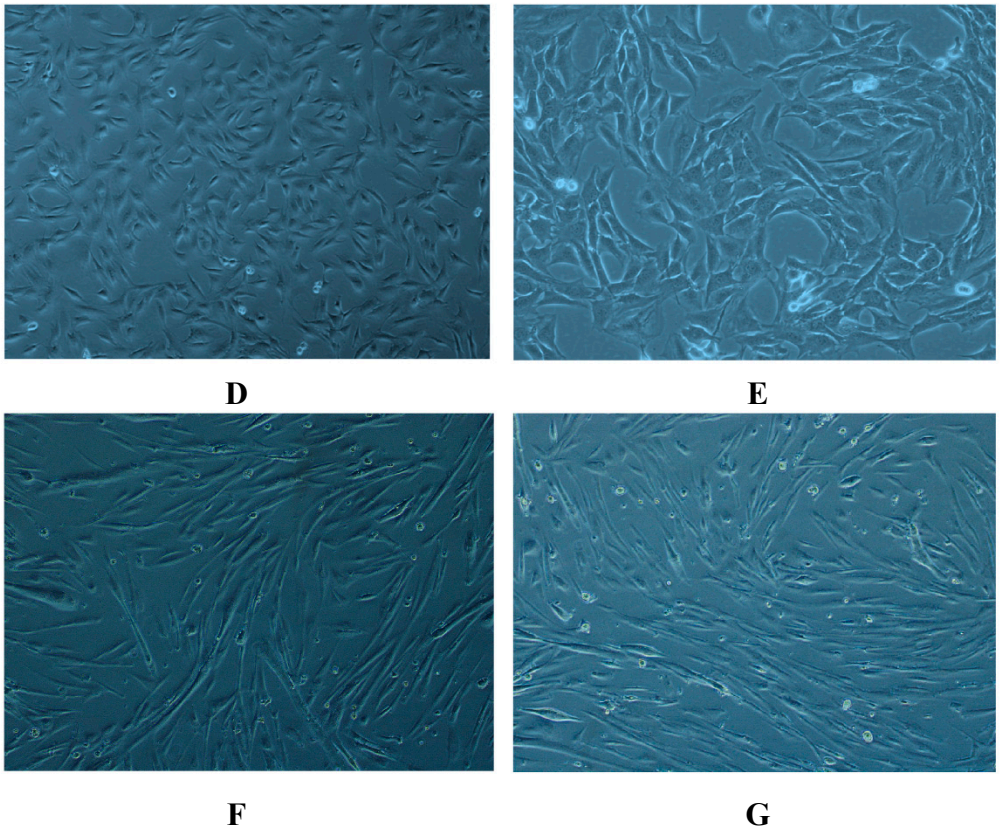


**Figure 1.** MTT cell viability assay on human skeletal muscle after AMA and celastrol treatment. Cell viability of AMA (**A**) and celastrol (**B**) was performed in a dose-dependent manner. The time-course evaluation of the optimal dose for AMA (30 μM) and celastrol (15 nM) was determined (**C**). Figures of the untreated cells (DMSO) (**D**), 30 μM AMA-treated cells (**E**), 15 nM celastrol-treated cell (**F**) and AMA-treated cells with 15 nM celastrol treatment (**G**) were taken at 40X magnification using fluorescence inverted microscope (Carl Zeiss, Göttingen, Germany). Figures represent one of three independent experiments. * $p < 0.05$ and ** $p < 0.01$ *vs*. untreated control.

### *2.2. Celastrol Increased Glucose Uptake in Insulin-Resistant Myotubes through the PI3K/Akt Pathway*

The impairments in glucose uptake and utilization are among the key events associated with mitochondrial dysfunction and insulin resistance [23,27]. We first investigated the effects of AMA alone on glucose uptake activity in human skeletal muscle using a $^{3}$H-2-DG uptake assay. As shown in Figure 2, cells under normal insulin-stimulated conditions (100 nM, 30 min) exhibited marked increase (50%, $p < 0.05$) in glucose uptake activity, compared to the basal level. However, AMA at a concentration of 30 μM was found to significantly decrease the basal (38%, $p < 0.05$) and insulin-stimulated glucose uptake activity (−78%, $p < 0.01$) compared to insulin-stimulated cells. This is in line with earlier findings that AMA treatment leads to impairment of glucose uptake activity in the cell [8]. Therefore, AMA treatment was used in the following experiments to induce mitochondrial dysfunction-induced insulin resistance in human skeletal muscle cells.

An evaluation of celastrol treatment alone on glucose uptake activity in human skeletal muscle was conducted. We found no significant changes in the basal glucose uptake activity for cells treated with

celastrol. Conversely, with insulin stimulation, celastrol significantly enhanced insulin-stimulated glucose uptake in AMA-treated cells, with an 86% ($p < 0.05$) increase in glucose uptake activity. These results may indicate that celastrol alone can be used as an insulin sensitizing agent for enhancement of glucose uptake activity in human skeletal muscle cells. Wortmannin, a potent PI3K-specific inhibitor, was utilized in the study to examine the mechanistic action of celastrol in regulating glucose uptake activity. Increasing evidence indicates that PI3K/Akt pathways are the key regulator of glucose metabolism and intracellular signaling activities relative to mitochondrial functions [28,29]. Co-incubation with wortmannin in human skeletal muscle diminished the glucose uptake activity in basal and insulin-stimulated conditions by −38% ($p < 0.05$) and −68% ($p < 0.01$), respectively, compared to untreated group.

Then, the effect of celastrol on AMA-treated cells was investigated. Co-treatment of celastrol on human skeletal muscle cells with mitochondrial dysfunction was investigated. The result showed that treatment with 15 nM celastrol on cells in the event of insulin stimulation significantly enhanced glucose uptake activity by +63% ($p < 0.05$) compared to AMA-treated cells. However, no significant difference was observed after celastrol treatment of AMA-treated cells at the basal level. Consequently, to evaluate whether the PI3K/Akt pathway is linked to celastrol-mediated improvements in glucose uptake activity, cells were pre-incubated with 100 nM wortmannin for 30 min before celastrol incubation. Co-treatment with wortmannin in insulin-resistant myotubes significantly diminished celastrol-induced insulin stimulation (−61%, $p < 0.05$) and basal (−18%, $p < 0.05$) glucose uptake activity (Figure 3B). These results indicated that celastrol treatment on skeletal muscle insulin resistance induced by AMA is modulated via PI3K/Akt pathways.

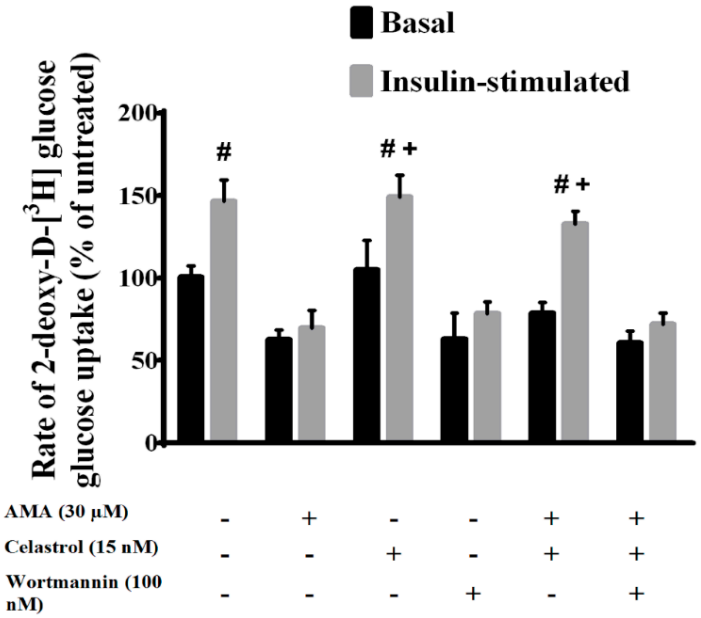


**Figure 2.** The mechanistic effects of AMA and celastrol treatment on the glucose uptake activity in skeletal muscle cells. Co-treatment with celastrol on skeletal muscle cells with mitochondrial dysfunction for 48 h improved insulin-mediated glucose uptake activity. However, wortmannin blocked this beneficial effects of celastrol on AMA-treated cells. # $p < 0.05$ *vs*. basal rate; + $p < 0.05$ *vs*. AMA-treated cells.

### *2.3. Celastrol Improves Mitochondrial Activity and Energy Production in AMA-Induced Insulin-Resistant Human Skeletal Muscle Cells*

The localization of the binding activity for inflammatory signaling NF-κB subunits p50 and p65 along with IκB were found in mitochondria, suggesting the involvement of this pathway in regulating mitochondrial activities [30]. Our earlier study demonstrated that NF-κB inhibition in adipocytes with insulin resistance led to the improvement of mitochondrial functions [23]. As celastrol has been reported to exhibit potent NF-κB inhibitors, we examined the mitochondrial functions of skeletal muscle cells after incubation with AMA and celastrol.

The energy production of the energetic tissues, including skeletal muscle, heart and liver, are mainly regulated by mitochondria in the form of chemical energy, known as adenosine triphosphate (ATP). In the present study (Figure 3A), insulin-treated cells exhibited with higher intracellular ATP concentrations (+200%, $p < 0.01$) than the basal group (untreated). AMA caused significant decrease in the intracellular ATP concentrations of both basal (−44%, $p < 0.05$) and insulin-stimulated (−70%, $p < 0.01$) cells. However, exposure to celastrol abolished this effect by elevating the intracellular ATP concentration levels of skeletal muscle cells in the absence (+46%, $p < 0.05$) and presence (+65%, $p < 0.05$) of insulin. Interestingly, treatment of human skeletal muscle with celastrol alone enhanced intracellular ATP content by +38% ($p < 0.01$) at the basal level while no significant effect was observed on the insulin-stimulated condition. Mitochondrial membrane integrity is one of the key indicators in determining normal cell function. Therefore, we examined whether celastrol affects mitochondrial membrane integrity (MMP). In brief, we measured the MMP using JC-1, a cationic dye that accumulates in mitochondria, and correlated it with the function of proton gradient. As depicted in Figure 3B, AMA treatment for 48 h decreased the MMP level by 58% ($p < 0.01$) relative to untreated cells. However, celastrol effectively recovered this detrimental effect of AMA by augmenting the level of MMP with a 42% increase ($p < 0.05$) compared to AMA-treated cells. Exposure to celastrol alone in cells revealed no significant changes to MMP levels compared to control (untreated).

To examine the association between mitochondrial dysfunction and ROS, the measurement of mitochondrial superoxide production was performed using a DCFDA assay kit. AMA caused a significant rise in ROS production (+125%, $p < 0.05$) while celastrol abolished this effect with an 84% ($p < 0.05$) decrease in mitochondrial superoxide production in human myotubes after 48 h (Figure 3C). In contrast, the previous report [22] showed that rapid treatment of celastrol on cardiomyoblast stimulates ROS production in 5–60 min. The difference in these observations is due to the different time point in measuring ROS production. In addition, we observed that celastrol treatment alone for 48 h revealed no changes to mitochondrial superoxide production levels relative to control.

Citrate synthase activity is commonly used as a marker of aerobic capacity and mitochondrial density in numerous energetic tissues such as skeletal muscle, liver and brain [31]. Following AMA treatment, we observed the reduced level (−65%, $p < 0.01$) of citrate synthase activity, which confirmed that AMA-induced mitochondrial dysfunction affects mitochondrial enzyme activity. Upon addition of celastrol, citrate synthase activity was significantly augmented (+53%, $p < 0.05$), as compared to AMA-treated cells (Figure 3D). A single treatment of human skeletal muscle cells with celastrol does not affect citrate synthase activity compared to control.

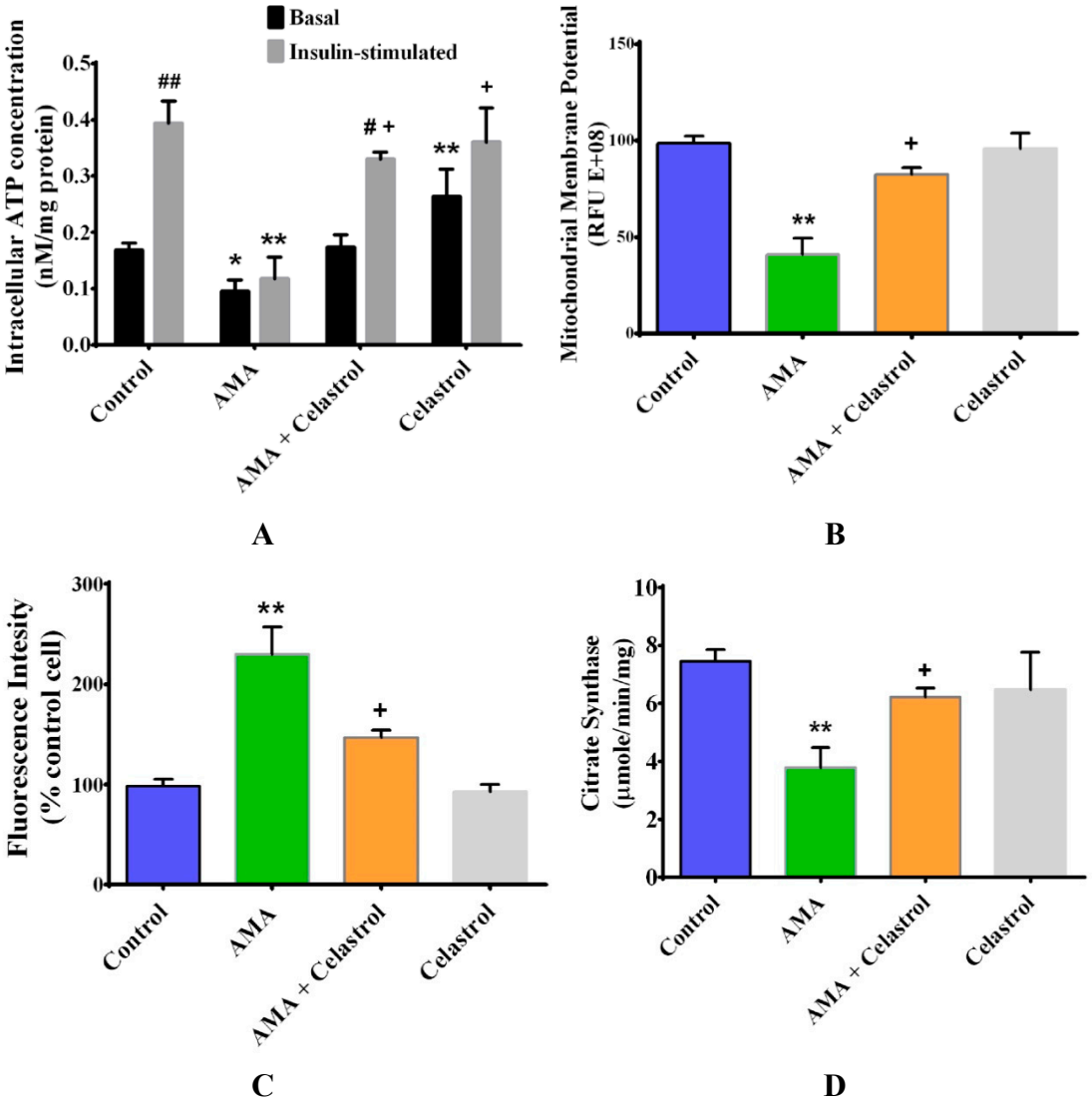


**Figure 3.** AMA and celastrol treatment of mitochondrial functions of skeletal muscle cells. After incubation, cells were assayed to measure intracellular ATP concentration (**A**), mitochondrial membrane potential (**B**), mitochondrial superoxide production (**C**) and citrate synthase activity (**D**). Basal and insulin-stimulated levels were shown. Basal rate refers to the rate of glucose transport in the absence of insulin. * $p < 0.05$ and ** $p < 0.01$ *vs*. untreated control; # $p < 0.05$ and ## $p < 0.01$ *vs*. basal rate; + $p < 0.05$ *vs*. AMA-treated cells.

### *2.4. Celastrol Attenuates Oxidative Stress in AMA-Treated Human Skeletal Muscle Cells*

There is growing evidence of the interplay relationship between oxidative stress and mitochondrial dysfunction in the progression of skeletal muscle insulin resistance [3,32]. Here, we examined the effects of celastrol on oxidative stress markers (including 8-OHdG DNA, protein carbonylation and lipid peroxidation) of AMA-treated human skeletal muscle cells. As depicted in Figure 4A–C, AMA significantly augmented the level of 8-OHdG DNA (+300%, $p < 0.01$), protein carbonyls (+160%, $p < 0.01$) and lipid peroxidation (+190%, $p < 0.01$) in human myotubes compared to untreated cells. Notably, all these deleterious impacts can be reversed by celastrol treatment. Relative to conditioned control, celastrol treatment alone showed no significant impact on the following parameters of the oxidative

stress level, except for lipid peroxidation, where celastrol significantly reduced the MDA level by −28% ($p < 0.05$).

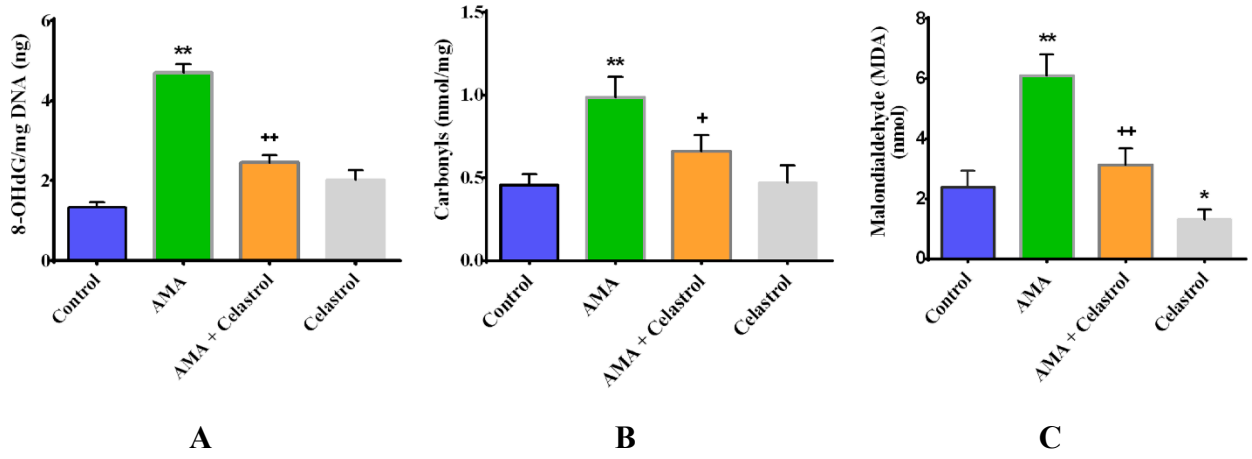


**Figure 4.** Effects of AMA and celastrol on the oxidative properties of human skeletal muscle. The quantification of 8-OHdG DNA (**A**), protein carbonyls (**B**) and lipid peroxidation levels (**C**) was determined after 30 μM AMA treatment with or without addition of 15 nM celastrol and celastrol treatment alone. Values are normalized against standard curves generated according to standard protocol provided by manufacturers. * $p < 0.05$ and ** $p < 0.01$ *vs*. untreated control; + $p < 0.05$ and ++ $p < 0.01$ *vs*. AMA-treated cells.

### *2.5. Celastrol Affects Mitochondrial Dynamics via Mitochondrial Fusion and Fission in AMA-Treated Skeletal Muscle Cells*

To further investigate the effects of AMA and celastrol on mitochondrial functions, we also measured the celastrol treatment of the expressions of mitochondrial fusion (mfn1 and mfn2) and fission (drp1) proteins. The result showed that AMA exposure to human myotubes upregulated the expression of mf1 and mfn2 proteins by 91% ($p < 0.01$) and 40% ($p < 0.05$), respectively. However, the presence of celastrol abrogated this aberrant effect by reducing the expression of mfn1 (−69%, $p < 0.05$) and mfn2 (−43%, $p < 0.05$) in human myotubes after 48 h of AMA treatment compared to control group. In line with this, drp1 protein level was partly reduced (−28%, $p < 0.05$) after AMA treatment but was amplified (+68%, $p < 0.01$) after pre-incubation with celastrol. (No significant changes were observed in the relative expression of mfn1, mfn2 and drp1 protein levels after treatment with 15 nM celastrol alone (Figure 5A–D).

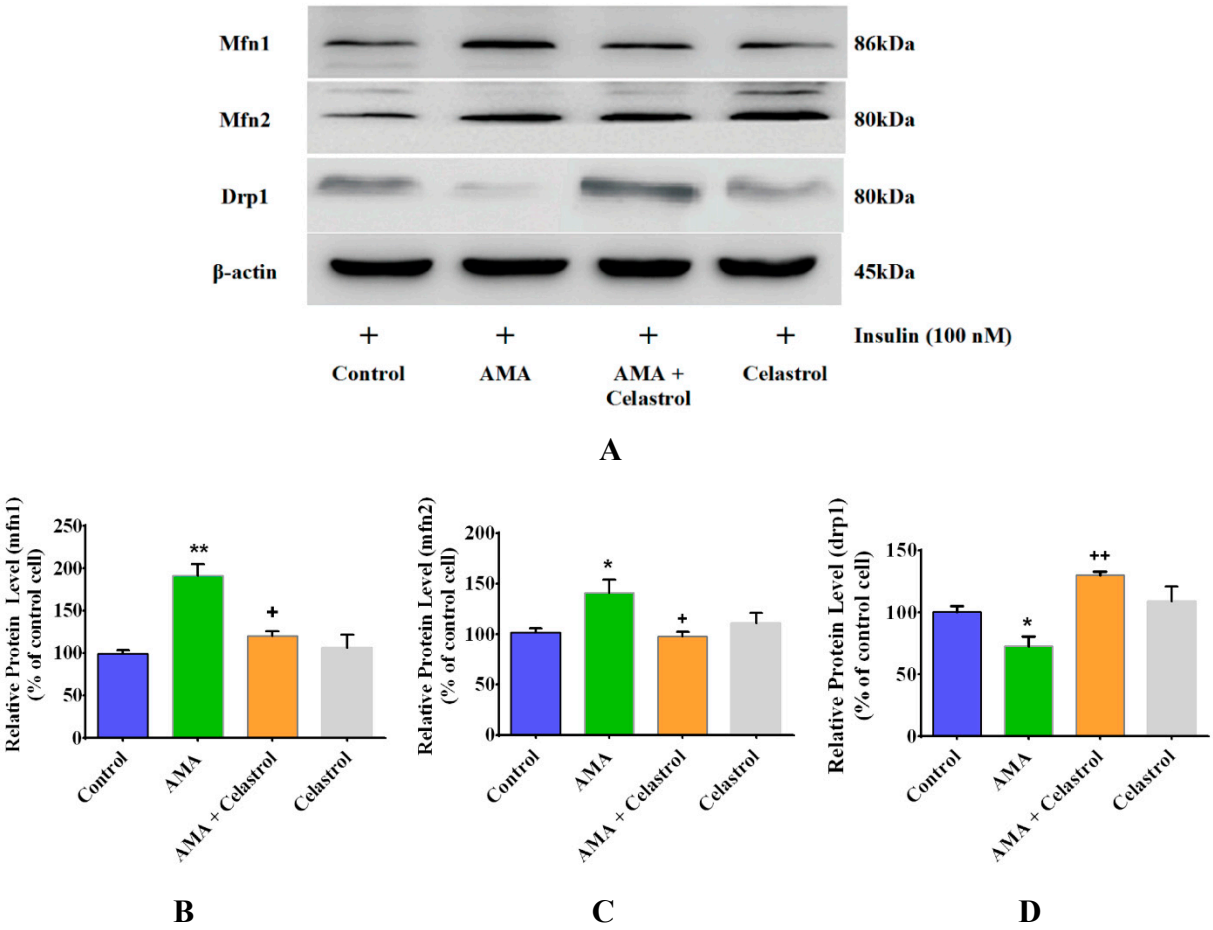


**Figure 5.** Effects of AMA and celastrol treatments on mitochondrial fusion and fission of human myotubes. Representative images of western blot analysis (**A**) on the relative expression of (**B**) mfn1, (**C**) mfn2 and (**D**) drp1 proteins were quantified with the corresponding antibodies using a densitometer. β-actin was used as loading control. Protein levels calculated by densitometry were normalized relative to β-actin signals. * $p < 0.05$ and ** $p < 0.01$ *vs*. untreated control; + $p < 0.05$ and ++ $p < 0.01$ *vs*. AMA-treated cells.

### *2.6. Effect of Celastrol on the Production of Pro-Inflammatory Cytokines IL-6, TNF-α and IL-1β in AMA-Induced Mitochondrial Dysfunction Human Skeletal Muscle Cells*

To examine whether the regulatory function of celastrol was associated with the activities of inflammatory cytokines, we measured the levels of IL-6, TNF-α and IL-1β using an ELISA-based assay. Interestingly, we found that AMA-treated cells exhibited augmented production of IL-6 (+280%, $p < 0.01$), TNF-α (+313%, $p < 0.01$) and IL-1β (+410%, $p < 0.01$) relative control cells. Upon co-incubation with celastrol, the amplified levels of IL-6, TNF-α and IL-1β were diminished by −157% ($p < 0.05$), −295% ($p < 0.01$) and −198% ($p < 0.05$) compared to AMA-treated cells as shown in Figure 6A–C. As a conditioned control, we co-incubated celastrol alone in human skeletal muscle cells. The result revealed that celastrol caused significant reduction (29%, $p < 0.05$) in TNF-α levels in normal human skeletal muscle cells while no significant changes were observed in the production of IL-6 and IL-1β.

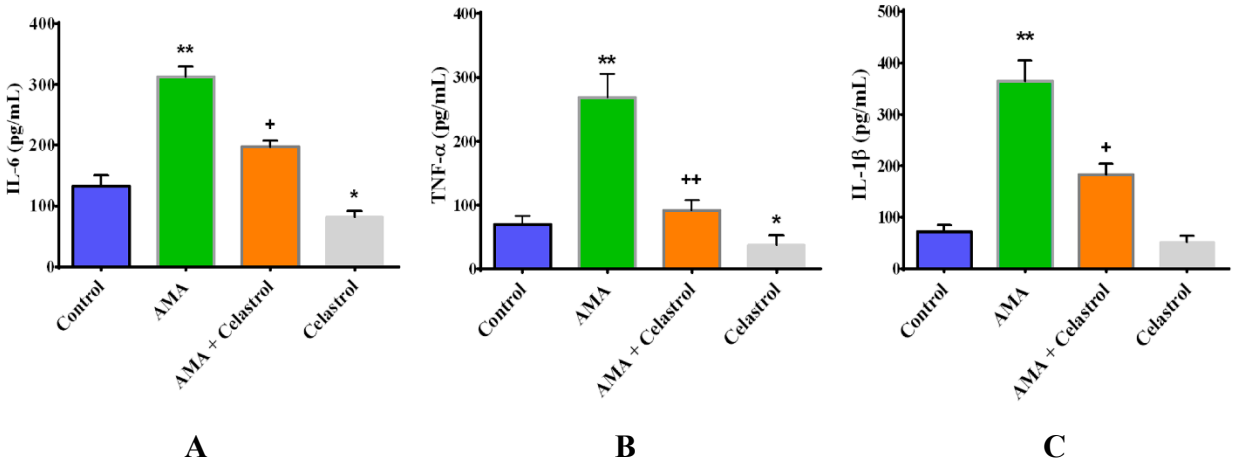


**Figure 6.** Effects of AMA and celastrol on the production of pro-inflammatory cytokines with regard to mitochondrial-induced insulin resistance in human myotubes. Cells were incubated for 48 h with DMSO (control), AMA, celastrol-AMA and celastrol only. The quantification of IL-6 (**A**), TNF-α (**B**) and IL-1β (**C**) was determined as briefly described in materials and methods. Values are normalized against standard curves generated according to standard protocols provided by manufacturers. * $p < 0.05$ and ** $p < 0.01$ *vs*. untreated control; + $p < 0.05$ and ++ $p < 0.01$ *vs*. AMA-treated cells.

### *2.7. Effect of AMA and Celastrol on NF-κB and IκBα Expression Protein Activity*

Next, we quantified the expression level of NF-κB (Ser-536) and IκBα (Ser-32) protein activity in human skeletal muscle cells after AMA treatment with or without celastrol. AMA significantly up-regulated NF-κB (+54%, $p < 0.05$) and IκBα (+69%, $p < 0.05$) protein expression activity (Figure 7A–C). Addition of 15 nM celastrol to these incubations attenuated the enhanced NF-κB phosphorylation (−56%, $p < 0.05$) and significantly blocked IκBα activity (−52%, $p < 0.05$) by inhibiting Ser-32 phosphorylation. Incubation with celastrol in normal cells exhibited no significant effect on the relative expression of NF-κB and IκBα protein activity even though celastrol has been reported to severely inhibit the expression of these proteins. This may suggest that the mechanistic effects of NF-κB inhibition in human skeletal muscle cells are selectively modulated in the event of mitochondrial dysfunction and metabolic stress.

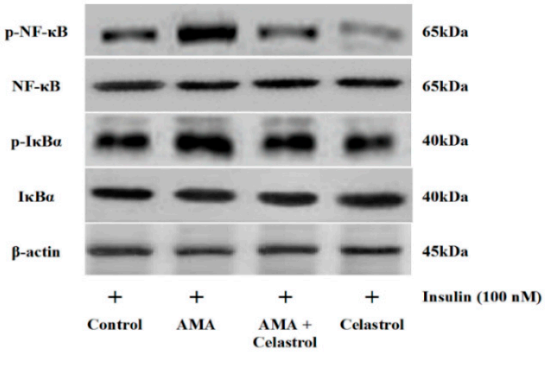


**Figure 7.** *Cont.*

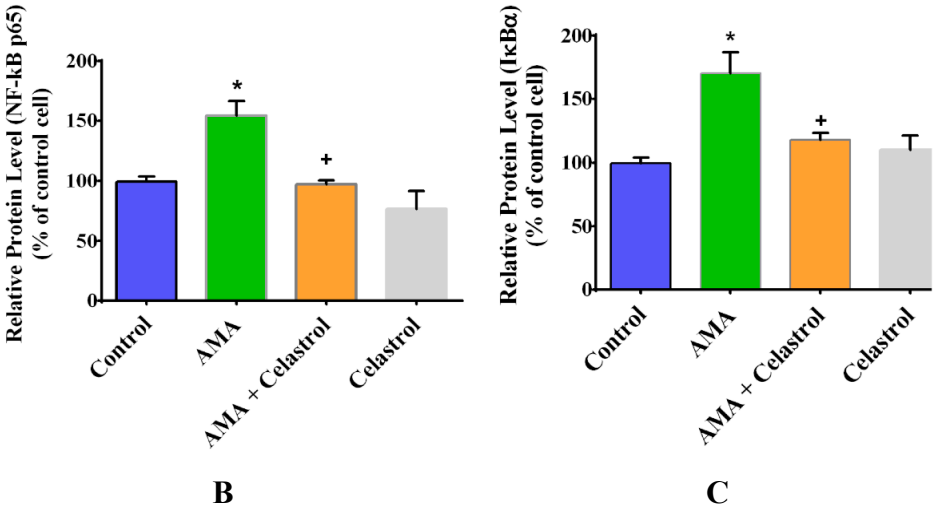


**Figure 7.** AMA treatment of human myotubes in the absence and presence of celastrol. Cells were grown in 6-well plates and treated with AMA and celastrol for 48 h. The representative images of western blot analysis (**A**) of the relative expression level of NF-κB (**B**) and IκBα (**C**) activity was measured and quantified. β-actin was used as a loading control. Protein levels calculated by densitometry were normalized relative to β-actin signals. * $p < 0.05$ *vs*. untreated control; + $p < 0.05$ *vs*. AMA-treated cells.

### *2.8. Effects of Celastrol on Protein Expression of Insulin Signaling Pathways and GLUT4 in AMA-Treated Human Skeletal Muscle Cells*

A number of downstream proteins targets of insulin signaling pathways including IRS1, Akt and AS160 have been postulated to play significant roles in insulin-stimulated glucose uptake [3,27]. In the present study, we examined the effects of celastrol on these downstream protein targets of human skeletal muscle cells treated with AMA. At 100 nM insulin stimulation, AMA-treated cells presented a significant reduced protein phosphorylation (all $p < 0.05$) of IRS1 (Tyr612) (−70%, Figure 8C), Akt (Ser473) (−74%, Figure 8D) and AS160 (Thr642) (−56% Figure 8E), compared to the insulin-treated control group. These AMA-induced reductions can be reversed by the addition of celastrol and resulted in significant increases (all $p < 0.05$) in protein phosphorylation of IRS1 (+45%), Akt (+63%) and AS160 (+45%).

To corroborate with abovementioned analysis, we further assessed the effect of AMA and celastrol on the relative expression of glucose transporter protein, GLUT4 relative to insulin stimulation (Figure 8B). Addition of AMA into the cultured human myotubes resulted to a significant reduction of GLUT4 protein expression with 66% ($p < 0.01$) compared to control group. Celastrol improved this impairment by elevating the expression of GLUT4 protein by 46% relative to AMA-treated human (Figure 8B,F). These data are consistent with the celastrol-induced increase in glucose uptake via significant enhancement of intracellular insulin signaling pathways.

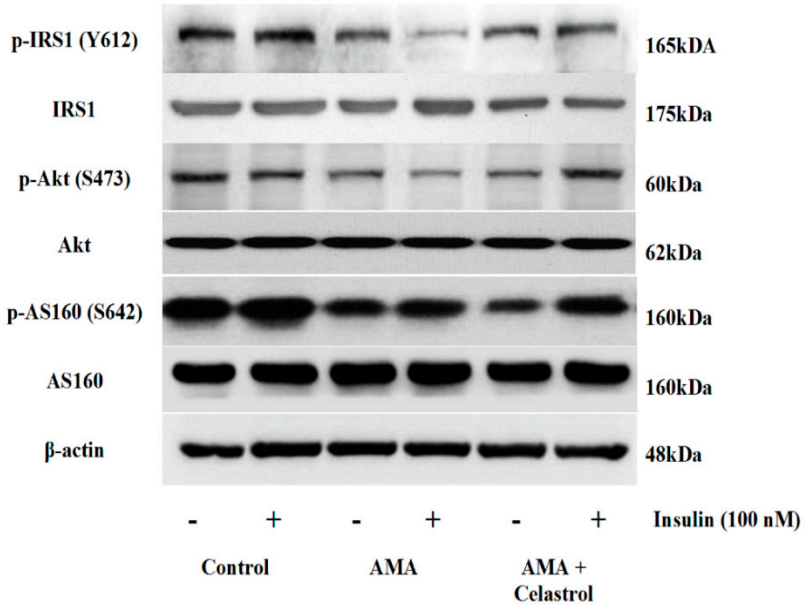


**A**

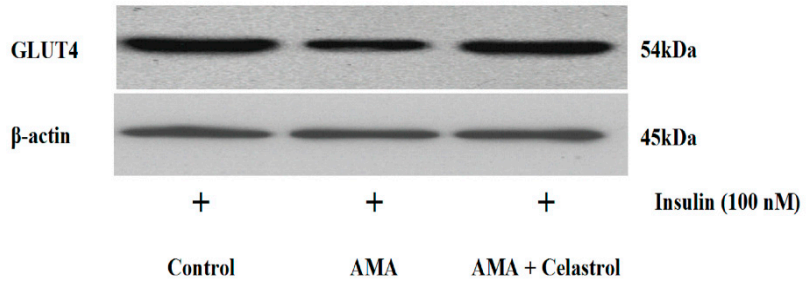


**B**

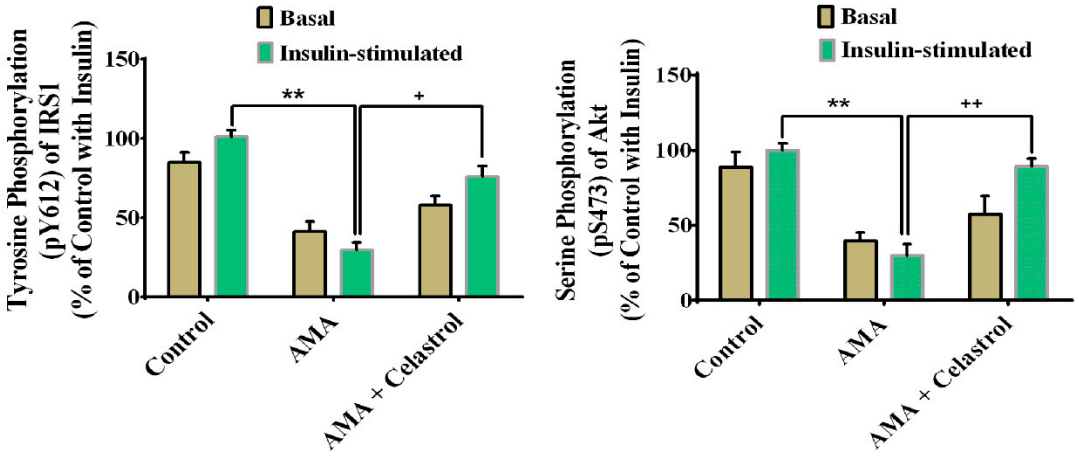


**C** **D**

**Figure 8.** *Cont.*

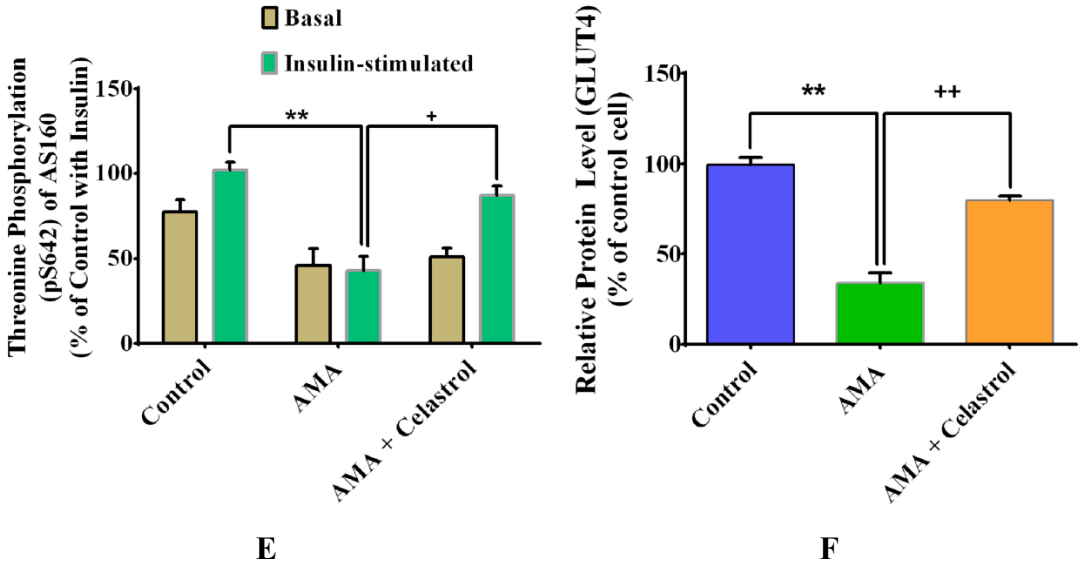


**Figure 8.** Effects of AMA and celastrol treatment on insulin signaling pathways and glucose transporters (GLUT4) of human myotubes. Cells were treated with AMA (30 μM) for 48 h before incubation with celastrol (15 nM). β-actin was used as an internal protein loading control. Protein levels for each corresponding antibody obtained from densitometry were normalized to the β-actin signal (**A**–**F**). * $p < 0.05$ and ** $p < 0.01$ *vs*. untreated control; # $p < 0.05$ *vs*. basal rate; + $p < 0.05$ and ++ $p < 0.01$ *vs*. AMA-treated cells.

### *2.9. Celastrol-Regulated pAMPK Expression and Inhibition of PKC θ in AMA-Treated Skeletal Muscle Cells*

The dysregulation of certain intracellular signaling pathways have been linked to the development of mitochondrial dysfunction and insulin resistance in a variety of insulin target tissues [3]. A reduced AMPK phosphorylation in skeletal muscle is also recognized as one of the key features of unhealthy cells with impaired lipid and glucose metabolism [33]. Long-term activation of PKC $\theta$ transcription factors is among the pivotal mechanisms involved in the event of skeletal muscle insulin resistance [34]. It would be interesting, therefore, to explore whether the ameliorative properties of celastrol affect these intracellular signaling pathways. Our study found that, compared with vehicle (control), AMA significantly diminished the level of phosphorylated AMPK (Thr-172) in the absence (−20%, $p < 0.05$) and presence (−70%, $p < 0.01$) of insulin. However, co-incubation with celastrol led to significant elevation of AMPK expression of AMA-treated cells (Figure 9A–B). As the stimulation of NF-κB signaling activity is correlated with the activation of PKC $\theta$, this prompted us to explore the correlative links between the roles of celastrol and regulation of PKC $\theta$ pathways. AMA exposure on human myotubes caused an increased phosphorylation expression (+51%, $p < 0.05$) of PKC $\theta$ (Ser-643/676) protein activity compared to untreated cells. Nevertheless, celastrol suppressed the effects of an AMA-induced increase of PKC $\theta$ activity by reducing the expression of PKC $\theta$ protein phosphorylation at the basal and insulin stimulation by −121% ($p < 0.01$) and −102% ($p < 0.01$), respectively, compared to AMA-treated cells. (Figure 9A–C).

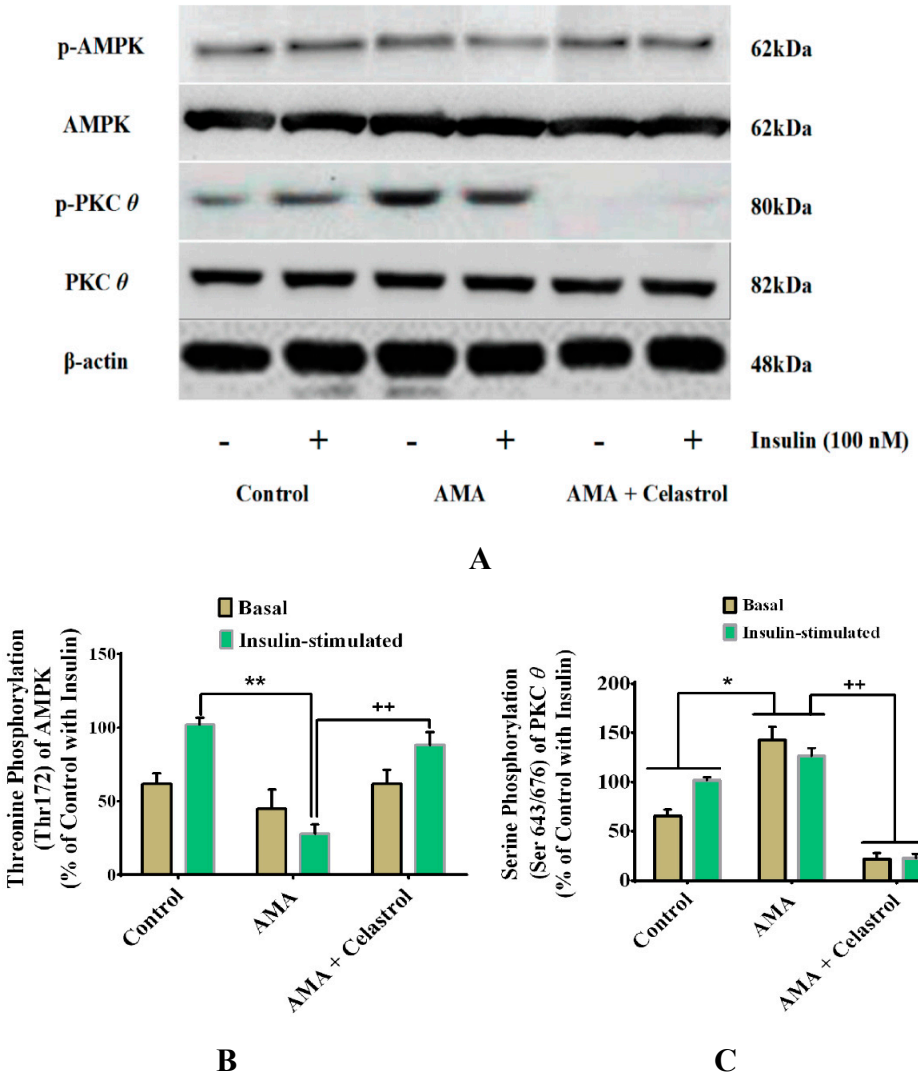


**Figure 9.** Effects of AMA and celastrol treatments on the protein expression of AMPK (Thr172) and PKC *θ* (Ser643/676) in human skeletal muscle-derived myoblast. Cells were cultured in media containing 30 μM AMA in the absence and presence of 15 nM celastrol for 48 h. Thereafter, cell lysates were subjected to western blot analysis (**A**). The percentage of specific and total protein phosphorylation was calculated to determine the relative level of exact amino acid residue phosphorylation (**A**–**C**). β-actin was used as internal protein loading control. Protein levels for each corresponding antibody obtained from densitometry were normalized to the β-actin signal. * $p < 0.05$ and ** $p < 0.01$ *vs*. untreated control; + $p < 0.05$ and ++ $p < 0.01$ *vs*. AMA-treated cells.

### *2.10. Discussion*

The evidence implicating the association between oxidative stress and inflammation in a number of peripheral tissues is correlative. However, the establishment of other *in vitro* phenotypes such as mitochondrial dysfunction-associated inflammation in skeletal muscle with insulin resistance has not been largely demonstrated. Correspondingly, there have been limited studies on the roles of inflammatory signaling pathways in the regulation of mitochondrial function. To our knowledge, the present study provides the first evidence in examining whether celastrol, a potent NF-κB inhibitor,

protects against mitochondrial dysfunction-induced insulin resistance in human skeletal muscle-derived myoblast. The current study supports the hypothesis that celastrol treatment attenuates the aberrant characteristics of skeletal muscle insulin resistance induced by deteriorated mitochondrial functions. The key findings of this study include the ability of celastrol to modulate intracellular insulin signaling pathways and its downstream effectors in the event of mitochondrial dysfunction in human skeletal muscle cells.

Insulin-stimulated glucose uptake assay is considered a "gold standard" in evaluating the degree of insulin resistance at the cellular level. It is generally believed that PI3K is the central regulatory axis pathway in intracellular insulin signaling cascades [35]. The activation of downstream effectors of IRS1 is predominantly dependent on the subsequent activation of the insulin receptor β subunit that leads to the stimulation of serine phosphorylation downstream of PI3K, known as Akt. The phosphorylation of Akt binding sites can promote GLUT4 translocation to cell membrane. Insulin signaling activities are known to be affected by mitochondrial dysfunction, oxidative stress and subsequent defects in other metabolic processes such as ATP contents, mitochondrial membrane potential, citrate synthase activity and ROS production [3,23]. This is supported by the fact that reduced oxidative phosphorylation rate, lower mitochondrial content and changes in mitochondrial dynamics of numerous peripheral tissues are related to the development of insulin resistance [36,37]. Moreover, it has been shown that impaired mitochondrial activities are linked to a disturbance in the relative function of mitochondrial dynamics [37,38]. This evidence implies that improvement of mitochondrial function may result in the improvement of peripheral and systemic insulin sensitivity as a whole. It was presumed that multiplication in ROS production serves to exacerbate oxidative stress mediated by augmented expression NF-κB binding activity [39]. Excess accumulation of pro-inflammatory cytokines in the event of mitochondrial dysfunction in normal human chondrocytes is linked to the overproduction of ROS and activation of NF-κB activities [40]. An integrative approach utilizing *in vitro* and *in vivo* studies discovered that high level of inflammatory gene expression due to enhanced binding sites of NF-κB activity was associated with mitochondrial $H_2O_2$ production-induced mitochondrial dysfunction [41,42]. The defects in mitochondrial respiration function with reduced ATP content in high-fat diet (HFD)-induced obese mice was accompanied by reduced expression of mfn1 and mfn2, while drp1 protein was significantly amplified when compared to the control group [43]. Additionally, it has been shown that the regulation of the Akt-mTOR-NF-κB signaling pathway in cardiomyocytes *in vitro* and *in vivo* is modulated via up-regulated mitochondrial fusions in the presence of insulin stimulation [28]. In this study, celastrol exhibits attributive properties via improvement of mitochondrial functions together with attenuated oxidative stress in AMA-treated skeletal muscle. This data suggests that celastrol may have potent effects on the improvement of mitochondrial functions in regards to the progression of insulin resistance in human skeletal muscle cells.

High levels of pro-inflammatory cytokines IL-6, TNF-α and IL-1β has been implicated with the progression of type 2 diabetes and glucose intolerance [44]. Here, we found that celastrol significantly abrogated the overwhelmed production of pro-inflammatory cytokines IL-6, TNF-α and IL-1β in AMA-treated cells. This observation is supported by previous reports showing that NF-κB transcription factors are responsible for mediating the expression of genes involved in the production of pro-inflammatory cytokines, chemokines and adhesion molecules [45]. As a potent inhibitor of NF-κB activity, celastrol may have had its effects on these pro-inflammatory genes and rescued human

myotubes from an insulin-resistant state. The present study suggests that the complex mechanism of celastrol could be regulated via synergistic enhancement of mitochondrial functions affecting oxidative metabolism and inflammatory response of the human skeletal muscle cells. The associative mechanism linking the development of mitochondrial dysfunction and inflammation is gaining attention [3,15]. NF-κB signaling activities have been proposed as one of the prominent pathways leading to the activation of inflammatory response in various cell types. Celastrol is a well-known potent inhibitor of NF-kB activation via *in vitro* and *in vivo* analyses [17,19,20,46–49]. Our result is consistent with earlier findings on the role of celastrol as a potent inhibitor of NF-κB and its nuclear translocation activity in a variety of cell types.

Insulin is an anabolic hormone that is released by the pancreas and serves to facilitate glucose uptake activity and glycogen storage in skeletal muscle. Excessive accumulation of intermediate lipid metabolites including DAG and ceramides activates serine kinase PKC $\theta$ and NF-κB transcription factors, thus promoting the inhibition of tyrosine phosphorylation via IRS1, AKT substrate of 160 kDa (AS160) and PI3K-related pathways. This process results in the diminished function of insulin signaling pathways, lessening the translocation of GLUT4 into the cell surface [50]. Oxidative stress and insulin resistance are closely associated with inflammation, evoking an inflammatory response via NF-κB and MAPK-mediated signaling [51]. The upsurge of ROS generation activates numerous inflammatory signaling pathways such as JNK and PKC and directly alters the inflammatory response in the peripheral tissues. The activation of intracellular signaling pathways by high levels of long-chain fatty acids and pro-inflammatory mediators enables the dissociation of NF-κB from inhibitors of IκB proteins for its translocation to the nucleus [52]. The subsequent activation of NF-κB boosts the transcription factors of various gene encoding inflammatory mediators such as IL-6 and TNF-α [53]. Elevated levels of these pro-inflammatory cytokines with boosted NF-κB activity may further mediate the activation and phosphorylation of intracellular signaling molecule JNK in skeletal muscle via inhibition of AS160 phosphorylation [54]. The excessive activation of serine phosphorylation of IRS1 by phosphorylated JNK (p-JNK) leads to the impairment of insulin signal transduction [55–57]. Prolonged activation of these inflammatory pathways results in the development of skeletal muscle insulin resistance [45]. In view of the involvement of mitochondrial dysfunction and oxidative stress-induced inflammation, the suppression of ROS production and inhibition of NF-κB-dependent inflammatory responses by celastrol in human skeletal muscle cells should be responsible for its beneficial regulation of IRS1-Akt-AS160 protein phosphorylation pathways. It is now becoming clear that celastrol produces an improvement to mitochondrial function of the human skeletal muscle cells with insulin resistance via enhanced intracellular insulin signaling pathways.

In the event of oxidative stress and mitochondrial dysfunction, previous studies showed that Complex I and III are the major sources of free-radical production [58]. Subsequently, this would result in the activation of serine/threonine phosphorylation on IRS-1, which in turn lead to the attenuation of IRS1 to activate PI3K and Akt [59]. Severe impairment in intracellular insulin signaling cascades may inherently inhibit translocation of GLUT4 to cell surface, so glucose uptake is reduced. The relative translocation of glucose transporters to the plasma membrane in the skeletal muscle has been recognized as one of key events in maintaining glucose homeostasis. It has been shown that the expression of GLUT4 protein level in skeletal muscle of type 2 diabetes subjects were reduced [60–62]. In the context of inflammatory signaling response, the participation of NF-κB signaling pathways in regulating GLUT4 mRNA

repression of skeletal muscle was first documented earlier [63]. In their study, there was an elevation of GLUT4 mRNA level in parallel to the reduced NF-κB activity in skeletal muscle of the fasted rats without insulin and glucose stimulation. Our finding substantiated the underlying mechanism on the effects of celastrol on the relative expression of GLUT4 protein and intracellular insulin signaling cascade events.

AMPK, a fuel sensing enzyme in present in numerous cell types, has been reported to exhibit a wide range of functions in regulating lipid and glucose metabolism in peripheral tissues. Pharmacological activation of this sensor promote the enhancement of fatty acid oxidation, mitochondrial biogenesis, GLUT4 translocation and insulin sensitivity [64,65]. Prolonged modification of cellular redox status, mitochondrial dysfunction and metabolic reprogramming are thought to be modulated via AMPK-mediated signaling pathways. It has been shown that AMPK activation can down-regulate the antagonistic effects of elevated pro-inflammatory cytokines IL-6 and IL-8 in human adipose tissue and skeletal muscle cells [66]. In view of that, one study showed that the expression level of NF-κB-p65 DNA-binding activity in myocytes from obese type 2 diabetes subjects was down-regulated following activation of AMPK by A769662 (activator of AMPK), but no effects on the insulin sensitivity of the cells were observed [67]. On the other hand, Barma and his colleagues found that the upsurge in the relative expression of NF-κB genes and proteins was mediated by phospho-PKC in insulin-resistant skeletal muscle cells [68]. High levels of NF-κB expression activity forced the cells to become insulin resistant. It has been observed that the transfer of phosphate group from PKC to NF-κB occurred in skeletal muscle cell free systems incubated with palmitate. Long chain fatty acids including palmitate have been shown to affect mitochondrial activity, insulin-stimulated glucose uptake and insulin signaling cascade events [3]. The present investigation indicates celastrol may have some attributive effects in transducing the level of the expression level of these proteins, thus preventing the development of mitochondrial dysfunction-induced insulin resistance in human skeletal muscle cells.

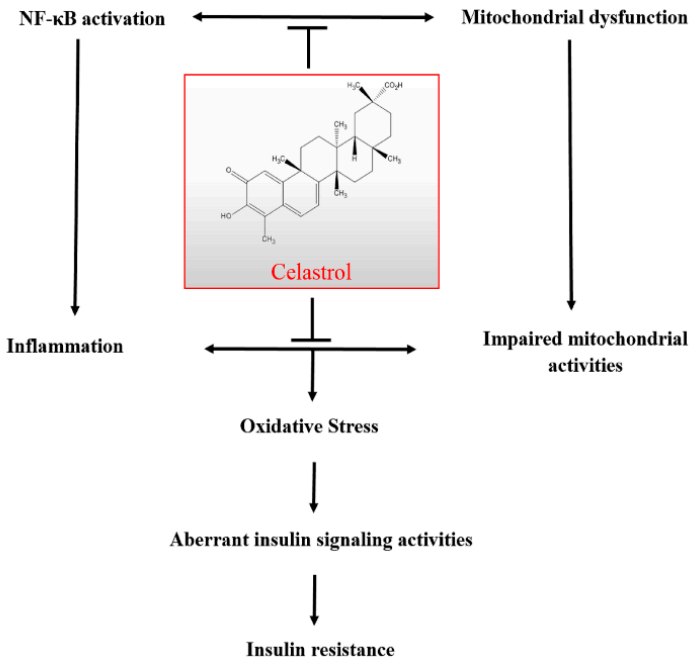


**Figure 10.** Schematic representation of the mechanistic action of celastrol on mitochondrial dysfunction-induced insulin resistance in human skeletal muscle cells.

It is known that celastrol can act as potent inhibitor of NF-κB signaling activities in various cell types [17,21,23,69]. In addition to its previous metabolic effects, the present investigation revealed that these unique characteristics of celastrol may have profound effects on a number of downstream pathways involving insulin sensitivity and glucose homeostasis of human skeletal muscle cells treated with AMA. As shown in Figure 10, we provide the first evidence that the mechanism underlying celastrol treatment in the event of mitochondrial dysfunction-induced insulin resistance is largely mediated through synergistic enhancement of mitochondrial functions and activation of anti-inflammatory pathways, leading to the metabolic improvement of intracellular signaling pathways in skeletal muscle insulin resistance. Nevertheless, the exact mechanism linking these metabolic improvements from celastrol in whole-body organisms against mitochondrial dysfunction-induced insulin resistance remains unclear, suggesting further investigation *in vivo* will be necessary to unravel these complex mechanisms.

## 3. Experimental Section

### *3.1. Cell Culture*

Human skeletal myoblasts (SKM102512A) were purchased from Zenbio Inc. and maintained at sub-confluence in skeletal muscle cell growth medium (SKM-M) (Zenbio Inc., Durham, NC, USA). The medium contains 1.0 g/L D-glucose Dulbecco's modified Engle's medium (DMEM) supplemented with fetal bovine serum, bovine serum albumin, fetuin, human insulin and antibiotics (penicillin, streptomycin and amphotericin B). The growth media were replaced every two days. Cells were incubated at 37 °C in a humidified atmosphere of 5% $CO_2$. Cells at passages 3–9 were used in all experiments of the current study. The 80%–90% confluent myoblasts were then washed with phosphate buffer saline (PBS), and differentiated to myotubes in skeletal muscle cell differentiation medium (SKM-D) (Zenbio Inc., Durham, NC, USA) with 10% of horse serum and antibiotics. Fresh differentiation media were added every 2–3 days. Myoblast were fused to form myotubes after 6 days of differentiation process, as presented by the appearance of elongated and multinucleated cells. The assays were performed accordingly on differentiated myotubes after seeding. The details of the donor and copy of certificate analysis provided by Zenbio Inc. is included in Supplementary 1.

### *3.2. AMA and Celastrol Treatment*

The induction of mitochondrial dysfunction and insulin resistance by AMA (Sigma, St. Louis, MO, USA) in human myotubes was performed as previously reported [70]. Cells were serum-starved for 18 h prior to the treatment at 37 °C in humidified 5% $CO_2$ atmosphere. After that, cells were incubated with AMA in order to induce impairment of mitochondrial complex III. Celastrol (purity >98%) was purchased from Sigma. Cells were treated with or without celastrol. Untreated cells with dimethyl sulfoxide (DMSO) and cells treated with celastrol alone were used as the conditioned controls in this study. Media in the controls and treated cells were replaced daily. All experiments were performed in triplicate.

### *3.3. Assessment of Cell Viability*

A quantitative colorimetric assay with 3-(4,5-dimethylthiazol-2-yl)-2,5-diphenyltetrazolium bromide (MTT) (Sigma) were utilized to determine the cell viability. Human myotubes were plated at a density

of $1 \times 10^5$ cells/well in skeletal muscle growth medium in a 96-well plate. Cells were then treated with varying concentration of AMA (10, 30, 50, 100 μM) with or without celastrol (5, 10, 20, 30 μM) in DMSO (vehicle). The final concentration of 0.1% DMSO (Sigma) was used. Accordingly, a stock concentration of AMA and celastrol was dissolved in DMSO. To ensure the integrity of myotubes functions, the optimal dose for each inhibitor that did not significantly affect cell viability was chosen for time-course assessment. The time-course evaluation was verified for each optimal dose (12, 24, 36 and 48 h). Briefly, after indicated treatment, media were removed and washed with PBS. A final concentration of 0.5 mg/mL of the MTT solution with the volume of 20 μL was added to each well and incubated for 5 h at 37 °C. Then, the MTT solution was removed and 200 μL of dimethyl sulfoxide (DMSO) was transferred into each well in order to form blue tetrazolium crystals. The absorbance of the final compounds was read at the wavelength of 570 nm and secondary wavelength of 630 nm using a ELISA plate reader (Erba LisaScan II, Mannheim, Germany).

### *3.4. Glucose Uptake Assay*

To investigate the roles of celastrol in AMA-treated human skeletal muscle cells, glucose uptake activity was carried out. The determination of glucose uptake activity rate (μmol/mg/min) in differentiated myotubes was performed by quantifying the radio-labeled glucose. Cells were first grown in 6-well plates in humidified 5% $CO_2$ at 37 °C. After exposure to 30 μM AMA for 24 h, cells were treated with 15 nM celastrol for another 24 h. Then, cells were washed twice with 1 mL/well serum-free DMEM for 4 h and immediately incubated with Krebs-Ringer HEPES (KRPH) buffer (118 mM NaCl, 5 mM KCl, 1.3 mM $CaCl_2$, 1.2 mM $MgSO_4$, 1.2 mM $KH_2PO_4$ and 30 mM HEPES, pH 7.4) for 30 min. For experiments involving insulin stimulation, cells were treated with 100 nM insulin for 30 min at 37 °C. Glucose uptake activity was measured by adding 2 μCi of 2-deoxy-D-[3H] glucose and 0.001 mM glucose in each well for 10 min at room temperature. After 60 min at 37 °C, cells were washed thrice with 3 mL/well of ice cold-PBS solution (pH 7.4) and glucose uptake activity was subsequently terminated. Then, cells were incubated and lysed with 0.7 mL of 1% Triton X-100 for 20 min at 37 °C. In order to quantify the incorporated radio-labeled glucose, the cell lysates were counted by using Tri-Carb 2700TR liquid scintillation counter (Packard Instrument Co., Meriden, CT, USA) [23].

### *3.5. Mitochondrial Superoxide Production*

Human myotubes were plated at $2.5 \times 10^5$ cells/well on black 96-well plates. After overnight growth, cells were washed with buffer solution. The production of cellular ROS was carried out by staining cells with 25 μM 2′,7′-dichlorofluorescin diacetate (DCFDA) (ab113851, Abcam) for 45 min at 37 °C. The media were removed and cells were washed two times with PBS. Thereafter, cells were treated with AMA with or without celastrol for 48 h. Cells were then collected and measured for fluorescence analysis utilizing a multimode plate reader (Promega, Madison, WI, USA) (excitation 485 nm, emission 535 nm).

### *3.6. Intracellular ATP Concentration*

Cells were treated with AMA in a 96-well white plate at 37 °C with or without celastrol for 48 h. The measurement of total intracellular ATP concentration was measured using a calorimetric ATP Assay Kit

32 (KA0806; Abnova Corporation, Walnut, CA, USA). In brief, 100 µL ATP Assay Buffers were used to lyse the cells in different wells. The deproteinization of cell lysates was performed by employing a 10 kDa Spin Column. The intracellular ATP concentration was calculated by comparing an ATP internal standard in both treated cells to the ratio of ATP content in untreated cells (control). The relative measurement of total intracellular ATP concentration were then measured with ELISA plate reader at the wavelength of 570 nm and normalized to protein concentrations.

### *3.7. Mitochondrial Membrane Potential (ΔΨm)*

The assessment of mitochondrial membrane potential (MMP) was assayed using the mitochondria-2 specific lipophilic cationic fluorescence dye 5,5′,6,6′-tetrachloro-1,1′,3,3′-tetraethylbenzimi-3 dazolylcarbocyanine iodide (JC-1) Detection Kit (KA1324; Abnova Corporation, Walnut, CA, USA) in accordance the manufacturer's instruction. This assay was performed in order to identify the changes in mitochondrial membrane potential relative to mitochondrial functions. Briefly, cells were seeded at $1 \times 10^6$ cells/well in a 96-well black culture plate for 48 h and co-incubated with AMA and celastrol. The media were aspirated and cells were washed three times with PBS. After that, 100 µL of JC-1 reagent was added into the wells followed by incubation in CO2 incubator at 37 °C for 30 min. The culture plate was centrifuged at the speed of 400× *g* for 5 min and supernatant was removed. The adherent cells were then washed twice with PBS and sufficient amount of PBS were added into each well to cover the cell layer. Thereafter, 100 µL of Assay Buffer was added to the wells and measured using a multimode plate reader (Promega). JC-1 aggregates fluoresced red (excitation 560 nm, emission 595 nm) in healthy cells with normal mitochondrial functions and high membrane potentials. In unhealthy cells with diminished membrane potential, JC-1 fluoresced green and formed a monomer in mitochondria of the cells.

### *3.8. Citrate Synthase Activity*

The mitochondrial citrate synthase activity was quantified in treated human myotubes at an immunocapture-based manner using Citrate Synthase Activity Assay Kit (ab119692) (Abcam, Cambridge, UK). Briefly, cells were grown in 96-well plate at $2.5 \times 10^5$ cells/well and treated with AMA before pre-incubation with celastrol. Cells were collected and centrifuged at the speed of 500× *g* for 10 min at 4 °C before washed with PBS. Then, cell pellets were solubilized at $2 \times 10^7$/mL in extraction buffer and incubated on ice for 2 min. Cell pellets were then centrifuged at 16,000× *g* for 20 min at the temperature of 4 °C. Pellets were discarded and supernatant was kept into clean tubes. The quantification of the protein in the extracts was performed using Pierce™ bicinchonic acid (BCA) protein assay kit (Life Technologies, Carlsbad, CA, USA). 100 µL of each diluted supernatant was added into well with an addition of a 1× Incubation Buffer as a zero standard. The aliquots were incubated for 3 h at room temperature. After incubation, the aliquots were aspirated and washed for two times before dispensing with 300 µL 1× Wash buffer into each well. The remaining buffer was removed and plate were inverted and blotted against clean paper towel to remove excess liquid. 100 µL of 1× Activity Solution was added into each well with minimization of bubble formation. The absorbance was recorded at a wavelength of 412 nM using an Elisa plate reader. The activity was expressed as µmol/min/mg protein.

### *3.9. Measurement of DNA Oxidative Damage, Protein Carbonylation and Lipid Peroxidation*

Biomarkers of oxidative stress were assayed to measure the oxidative metabolism of the cells. Quantification of 8-hydroxydeoxyguanosine (8-OHdG) was determined using the OxiSelectTM Oxidative DNA Damage ELISA Kit (Cell Biolabs, San Diego, CA, USA) following the maker's instructions. The relative level of protein carbonylation in cell lysate was measured using a Protein Carbonyl Content Assay Kit (Cayman Chemical, Ann Arbor, MI, USA) and lipid peroxidation was estimated using Lipid Peroxidation (MDA) Assay Kit (Sigma), as previously described. All assays were performed in triplicate and measured calorimetrically using an ELISA plate reader.

### *3.10. Cytokine ELISA for IL-6, TNF-α and IL-1β*

Cells were seeded in 96-well white plates in humidified 5% $CO_2$ at 37 °C. The quantitative measurement of the relative concentrations of pro-inflammatory cytokines IL-6, TNF-α and IL-1β in conditioned media of human myotubes with or without treatment were analyzed using a commercial ELISA kit (Invitrogen, Carlsbad, CA, USA), following the user guide provided with the kit. The minimum detectable concentration level were 7 pg/mL for IL-1β and 3 pg/mL for both Il-6 and TNF-α. The relative concentration of these pro-inflammatory cytokines was obtained from the standard curve and expressed as per mg of total extractable cell protein.

### *3.11. Western Immunoblotting*

Immunoblotting analysis was carried out as previously reported [23]. Human myotubes were cultured on a 6-well plate and serum-starved for 8 h before incubated with AMA and celastrol accordingly for 48 h. In brief, after treatments, cells were washed twice with ice cold-PBS and Krebs-Ringer HEPES buffer. Cells were then homogenized with protein lysis buffer (50 mM Tris pH7.5, 1 mM EDTA, 1 mM EGTA, 10% glycerol, 1% triton X-100, 50 mM NaF, 5 mM $Na_4P_2O_7$, 1 mM $Na_3VO_4$, 1 mM DTT) containing protease and phosphatase inhibitors cocktails (1:1000). After being incubated on ice for 30 min, the extraction of total and phosphorylated protein from cell lysates was performed by differential centrifugation at the speed of 20,000× *g* for 20 min at 4 °C. Protein concentration was quantified in triplicate using the Pierce™ BCA protein assay kit in accordance with the standard protocol provided by the supplier (Thermo Scientific, Waltham, Massachusetts, USA). The aliquots of each cell lysate (25 μg) were subjected to odecyl sulfate-polyacrylamide gel electrophoresis (SDS-PAGE) and directly transferred to nitrocellulose membranes (Whatman, London, UK). Following a blocking step in Tris-buffered saline/Tween-20 (TBST) containing 5% *w*/*v* bovine serum albumin (BSA) for 1 hour at room temperature, the membranes were hybridized with the following primary antibodies at 4 °C overnight. The secondary antibody was incubated for 1 hour at the same temperature in the dark. The membranes and following primary antibodies were diluted overnight in TBST: p-NF-κB p65 (Ser-536) (1:1000, Cell Signaling Technology, Danvers, MA, USA), p-IκBα (Ser-32) (1:1000, Cell Signaling Technology) FOXO1 (1:1000, Cell Signaling Technology), mfn1 (1:1000, Santa Cruz Biotechnology, Santa Cruz, CA, USA), mfn2 (1:1000, 32 Santa Cruz Biotechnology), drp1 (1:1000, Santa Cruz Biotechnology), pY612-IRS1 (1:1000, Upstate Biotechnology, Lake Placid, NY, USA), IRS1 (1:1000, Upstate Biotechnology), pS473-Akt (1:1000, Cell Signaling Technology), Akt (1:1000, Cell Signaling

Technology), pS462 AS160 (1:1000, Cell Signaling Technology), AS160 (1:1000, Cell Signaling Technology), pPKC $\theta$ (1:1000, Santa Cruz), PKC $\theta$ (1:1000, Santa Cruz Biotechnology), pAMPK (1:1000, Santa Cruz Biotechnology), AMPK (1:1000, Santa Cruz Biotechnology), GLUT4 (1:1000, 35 Cell Signaling Technology) and β-actin (1:1000, Cell Signaling Technology) at room temperature. The blots were then washed with TBST at a dilution of 1:10000 for 1 hour at room temperature before incubation with appropriate anti-rabbit horseradish peroxidase (HRP)-conjugated secondary antibodies (1: 5000) (Life Technologies, Carlsbad, CA, USA). For experiments involving protein phosphorylation, cells were stimulated with 100 nM insulin for 10 min, lysed and immuno-precipitated as previously described [71]. The blots were developed by chemiluminescence using ECL plus kits (Amersham, Piscataway, NJ, USA), visualized using ChemiDocTM XRS + with Image Lab$^{TM}$ software. The quantification of protein bands was quantified using a standard densitometry. The immunoblotting experiments were performed in triplicate.

### *3.12. Statistical Analysis*

All experimental data were shown as means ± standard error of the mean (SEM) of the indicated sample size (n)—for a minimum of three cell culture experiments. Comparison between groups was performed using one-way ANOVA with a Tukey post-hoc test or Duncan's multiple range tests as appropriate; $p < 0.05$ was considered statistically significant. Analyses were carried out using the SPSS 16.0 software package.

## 4. Conclusions

In summary, the present study has provided insights into the protective roles of celastrol in mitochondrial dysfunction and insulin resistance in human skeletal muscle-derived myoblast. In addition to its roles in inhibiting inflammatory signaling, celastrol improved glucose uptake and mitochondrial function and enhanced intracellular insulin signaling activities and its downstream targets in AMA-treated human skeletal muscle cells. The current study, together with published findings, suggests that celastrol is a potential therapeutic molecule for protection against mitochondrial dysfunction and insulin resistance.

## Acknowledgments

The authors gratefully acknowledge financial and technical support from the Ministry of Education, Malaysia, under Fundamental Research Grant Scheme (FRGS-2013-2015) and Universiti Teknologi Malaysia (Vot. No. R.J130000.7809.4F284). Mohamad Hafizi Abu Bakar is financially sponsored by the "UTM Doctoral Zamalah Award" from Universiti Teknologi Malaysia.

## Author Contributions

Mohamad Hafizi Abu Bakar designed and performed the experiments, analyzed the data and wrote the paper. Kian-Kai Cheng, Mohamad Roji Sarmidi, Harisun Yaakob and Hasniza Zaman Huri participated in the interpretation of data and gave final approval of the paper to be submitted with a critical revision.

## Conflicts of Interest

All authors declare no conflict of interest.

## References


1. *IDF Diabetes Atlas*, 6th ed.; International Diabetes Federation: Brussels, Belgium, 2013; p. 160.
2. Abu Bakar, M.H.; Sarmidi, M.R.; Cheng, K.K.; Ali Khan, A.; Chua, L.S.; Zaman Huri, H.; Yaakob, H. Metabolomics-The Complementary Field in Systems Biology: A Review on Obesity and Type 2 Diabetes. *Mol. Biosyst.* **2015**, doi:10.1039/C5MB00158G.
3. Hafizi Abu Bakar, M.; Kian Kai, C.; Wan Hassan, W.N.; Sarmidi, M.R.; Yaakob, H.; Zaman Huri, H. Mitochondrial dysfunction as a central event for mechanisms underlying insulin resistance: The roles of long chain fatty acids. *Diabetes Metab. Res. Rev.* **2014**, doi:10.1002/dmrr.2601.
4. Bondia-Pons, I.; Ryan, L.; Martinez, J.A. Oxidative stress and inflammation interactions in human obesity. *J. Physiol. Biochem.* **2012**, *68*, 701–711.
5. Petersen, K.F.; Dufour, S.; Befroy, D.; Garcia, R.; Shulman, G.I. Impaired Mitochondrial Activity in the Insulin-Resistant Offspring of Patients with Type 2 Diabetes. *N. Engl. J. Med.* **2004**, *350*, 664–671.
6. Gaster, M.; Rustan, A.C.; Aas, V.; Beck-Nielsen, H. Reduced Lipid Oxidation in Skeletal Muscle From Type 2 Diabetic Subjects May Be of Genetic Origin: Evidence From Cultured Myotubes . *Diabetes* **2004**, *53*, 542–548.
7. Szendroedi, J.; Phielix, E.; Roden, M. The role of mitochondria in insulin resistance and type 2 diabetes mellitus. *Nat. Rev. Endocrinol.* **2012**, *8*, 92–103.
8. Wang, C.H.; Wang, C.C.; Wei, Y.H. Mitochondrial dysfunction in insulin insensitivity: Implication of mitochondrial role in type 2 diabetes. *Ann. N. Y. Acad. Sci.* **2010**, *1201*, 157–165.
9. Martins, A.R.; Nachbar, R.T.; Gorjao, R.; Vinolo, M.A.; Festuccia, W.T.; Lambertucci, R.H.; Cury-Boaventura, M.F.; Silveira, L.R.; Curi, R.; Hirabara, S.M. Mechanisms underlying skeletal muscle insulin resistance induced by fatty acids: Importance of the mitochondrial function. *Lipids Health Dis.* **2012**, *11*, 30.
10. Zhang, H.; Zhang, H.M.; Wu, L.P.; Tan, D.X.; Kamat, A.; Li, Y.Q.; Katz, M.S.; Abboud, H.E.; Reiter, R.J.; Zhang, B.X. Impaired mitochondrial complex III and melatonin responsive reactive oxygen species generation in kidney mitochondria of db/db mice. *J. Pineal Res.* **2011**, *51*, 338–344.
11. Chattopadhyay, M.; Guhathakurta, I.; Behera, P.; Ranjan, K.R.; Khanna, M.; Mukhopadhyay, S.; Chakrabarti, S. Mitochondrial bioenergetics is not impaired in nonobese subjects with type 2 diabetes mellitus. *Metabolism* **2011**, *60*, 1702–1710.
12. Lanza, I.R.; Sreekumaran Nair, K. Regulation of skeletal muscle mitochondrial function: Genes to proteins. *Acta Physiol.* **2010**, *199*, 529–547.
13. Roden, M. How Free Fatty Acids Inhibit Glucose Utilization in Human Skeletal Muscle. *Physiology* **2004**, *19*, 92–96.
14. Yuzefovych, L.V; Schuler, A.M.; Chen, J.; Alvarez, D.F.; Eide, L.; LeDoux, S.P.; Wilson, G.L.; Rachek, L.I. Alteration of mitochondrial function and insulin sensitivity in primary mouse skeletal muscle cells isolated from transgenic and knockout mice: Role of OGG1. *Endocrinology* **2013**, doi:10.1210/en.2013-1076.

15. Hernández-Aguilera, A.; Rull, A.; Rodríguez-Gallego, E.; Riera-Borrull, M.; Luciano-Mateo, F.; Camps, J.; Menéndez, J.A.; Joven, J. Mitochondrial Dysfunction: A Basic Mechanism in Inflammation-Related Non-Communicable Diseases and Therapeutic Opportunities. *Mediat. Inflamm.* **2013**, *2013*, Article ID 135698.
16. Morita, T. Celastrol: A New Therapeutic Potential of Traditional Chinese Medicine. *Am. J. Hypertens.* **2010**, *23*, 821.
17. Lee, J.-H.; Koo, T.H.; Yoon, H.; Jung, H.S.; Jin, H.Z.; Lee, K.; Hong, Y.S.; Lee, J.J. Inhibition of NF-κB activation through targeting IκB kinase by celastrol, a quinone methide triterpenoid. *Biochem. Pharmacol.* **2006**, *72*, 1311–1321.
18. Sethi, G.; Ahn, K.S.; Pandey, M.K.; Aggarwal, B.B. Celastrol, a novel triterpene, potentiates TNF-induced apoptosis and suppresses invasion of tumor cells by inhibiting NF-κB–regulated gene products and TAK1-mediated NF-κB activation. *Blood* **2006**, *109*, 2727–2735.
19. Shao, L.; Zhou, Z.; Cai, Y.; Castro, P.; Dakhov, O.; Shi, P.; Bai, Y.; Ji, H.; Shen, W.; Wang, J. Celastrol Suppresses Tumor Cell Growth through Targeting an AR-ERG-NF-κB Pathway in TMPRSS2/ERG Fusion Gene Expressing Prostate Cancer. *PLoS ONE* **2013**, *8*, e58391.
20. Kim, J.E.; Lee, M.H.; Nam, D.H.; Song, H.K.; Kang, Y.S.; Lee, J.E.; Kim, H.W.; Cha, J.J.; Hyun, Y.Y.; Han, S.Y.; *et al*. Celastrol, an NF-κB Inhibitor, Improves Insulin Resistance and Attenuates Renal Injury in db/db Mice. *PLoS ONE* **2013**, *8*, e62068.
21. Yu, X.; Tao, W.; Jiang, F.; Li, C.; Lin, J.; Liu, C. Celastrol Attenuates Hypertension-Induced Inflammation and Oxidative Stress in Vascular Smooth Muscle Cells via Induction of Heme Oxygenase-1. *Am. J. Hypertens.* **2010**, *23*, 895–903.
22. Der Sarkissian, S.; Cailhier, J.-F.; Borie, M.; Stevens, L.M.; Gaboury, L.; Mansour, S.; Hamet, P.; Noiseux, N. Celastrol protects ischaemic myocardium through a heat shock response with up-regulation of haeme oxygenase-1. *Br. J. Pharmacol.* **2014**, *171*, 5265–5279.
23. Abu Bakar, M.H.; Sarmidi, M.R.; Kian Kai, C.; Zaman Huri, H.; Yaakob, H. Amelioration of Mitochondrial Dysfunction-Induced Insulin Resistance in Differentiated 3T3-L1 Adipocytes via Inhibition of NF-κB Pathways. *Int. J. Mol. Sci.* **2014**, *15*, 22227–22257.
24. Kang, S.W.; Kim, M.S.; Kim, H.S.; Kim, Y.; Shin, D.; Park, J.H. Y.; Kang, Y.H. Celastrol attenuates adipokine resistin-associated matrix interaction and migration of vascular smooth muscle cells. *J. Cell. Biochem.* **2013**, *114*, 398–408.
25. Ju, S.M.; Cho, Y.S.; Park, J.S. Celastrol ameliorates cytokine toxicity and pro-inflammatory immune responses by suppressing NF-kB activation in RINm5F beta cells. *Biochem. Mol. Biol. Rep.* **2015**, *48*, 172–177.
26. Hansen, J.; Palmfeldt, J.; Vang, S.; Corydon, T.J.; Gregersen, N.; Bross, P. Quantitative Proteomics Reveals Cellular Targets of Celastrol. *PLoS ONE* **2011**, *6*, e26634.
27. Wang, C.H.; Wang, C.C.; Huang, H.C.; Wei, Y.H. Mitochondrial dysfunction leads to impairment of insulin sensitivity and adiponectin secretion in adipocytes. *FEBS J.* **2013**, *280*, 1039–1050.
28. Parra, V.; Verdejo, H.E.; Iglewski, M.; del Campo, A.; Troncoso, R.; Jones, D.; Zhu, Y.; Kuzmicic, J.; Pennanen, C.; Lopez-Crisosto, C.; *et al*. Insulin Stimulates Mitochondrial Fusion and Function in Cardiomyocytes via the Akt-mTOR-NFκB-Opa-1 Signaling Pathway. *Diabetes* **2014**, *63*, 75–88.
29. Schultze, S.M.; Hemmings, B.A.; Niessen, M.; Tschopp, O. PI3K/AKT, MAPK and AMPK signalling: Protein kinases in glucose homeostasis. *Expert Rev. Mol. Med.* **2012**, *14*, e1.

30. Cogswell, P.C.; Kashatus, D.F.; Keifer, J.A.; Guttridge, D.C.; Reuther, J.Y.; Bristow, C.; Roy, S.; Nicholson, D.W.; Baldwin, A.S. NF-κB and IκBα Are Found in the Mitochondria: Evidence for Regulation of Mitochondrial Gene Expression by NF-κB. *J. Biol. Chem.* **2003**, *278*, 2963–2968.
31. Larsen, S.; Nielsen, J.; Hansen, C.N.; Nielsen, L.B.; Wibrand, F.; Stride, N.; Schroder, H.D.; Boushel, R.; Helge, J.W.; Dela, F.; *et al*. Biomarkers of mitochondrial content in skeletal muscle of healthy young human subjects. *J. Physiol.* **2012**, *590*, 3349–3360.
32. Pagel-Langenickel, I.; Bao, J.; Pang, L.; Sack, M.N. The role of mitochondria in the pathophysiology of skeletal muscle insulin resistance. *Endocr. Rev.* **2010**, *31*, 25–51.
33. Gruzman, A.; Babai, G.; Sasson, S. Adenosine Monophosphate-Activated Protein Kinase (AMPK) as a New Target for Antidiabetic Drugs: A Review on Metabolic, Pharmacological and Chemical Considerations. *Rev. Diabet. Stud.* **2009**, *6*, 13–36.
34. Li, Y.; Soos, T.J.; Li, X.; Wu, J.; DeGennaro, M.; Sun, X.; Littman, D.R.; Birnbaum, M.J.; Polakiewicz, R.D. Protein Kinase C θ Inhibits Insulin Signaling by Phosphorylating IRS1 at Ser1101. *J. Biol. Chem.* **2004**, *279*, 45304–45307.
35. Choi, K.; Kim, Y.B. Molecular mechanism of insulin resistance in obesity and type 2 diabetes. *Korean J. Intern. Med.* **2010**, *25*, 119–129.
36. Højlund, K.; Mogensen, M.; Sahlin, K.; Beck-Nielsen, H. Mitochondrial Dysfunction in Type 2 Diabetes and Obesity. *Endocrinol. Metab. Clin. North Am.* **2008**, *37*, 713–731.
37. Shenouda, S.M.; Widlansky, M.E.; Chen, K.; Xu, G.; Holbrook, M.; Tabit, C.E.; Hamburg, N.M.; Frame, A.A.; Caiano, T.L.; Kluge, M.A.; *et al*. Altered mitochondrial dynamics contributes to endothelial dysfunction in diabetes mellitus. *Circulation* **2011**, *124*, 444–453.
38. Jheng, H.F.; Tsai, P.J.; Guo, S.M.; Kuo, L.H.; Chang, C.S.; Su, I.J.; Chang, C.R.; Tsai, Y.S. Mitochondrial fission contributes to mitochondrial dysfunction and insulin resistance in skeletal muscle. *Mol. Cell. Biol.* **2012**, *32*, 309–319.
39. Mariappan, N.; Elks, C.M.; Sriramula, S.; Guggilam, A.; Liu, Z.; Borkhsenious, O.; Francis, J. NF-κB-induced oxidative stress contributes to mitochondrial and cardiac dysfunction in type II diabetes. *Cardiovasc. Res.* **2010**, *85*, 473–483.
40. Vaamonde-García, C.; Valcarcel-Ares, N.; Riveiro-Naveira, R.; Lema, B.; Blanco, F.J.; López-Armada, M.J. Inflammatory response is modulated by mitochondrial dysfunction in cultured normal human chondrocytes. *Ann. Rheum. Dis.* **2010**, *69*, A15–A16.
41. Ungvari, Z.; Orosz, Z.; Labinskyy, N.; Rivera, A.; Xiangmin, Z.; Smith, K.; Csiszar, A. Increased mitochondrial H2O2 production promotes endothelial NF-κB activation in aged rat arteries. *Am. J. Physiol. Hear. Circ. Physiol.* **2007**, *293*, H37–H47.
42. Vaamonde-García, C.; Riveiro-Naveira, R.R.; Valcárcel-Ares, M.N.; Hermida-Carballo, L.; Blanco, F.J.; López-Armada, M.J. Mitochondrial dysfunction increases inflammatory responsiveness to cytokines in normal human chondrocytes. *Arthritis Rheum.* **2012**, *64*, 2927–2936.
43. Liu, R.; Jin, P.; LiqunYu; Wang, Y.; Han, L.; Shi, T.; Li, X. Impaired Mitochondrial Dynamics and Bioenergetics in Diabetic Skeletal Muscle. *PLoS ONE* **2014**, *9*, e92810.
44. Guest, C.B.; Park, M.J.; Johnson, D.R.; Freund, G.G. The implication of proinflammatory cytokines in type 2 diabetes. *Front. Biosci.* **2008**, *13*, 5187–5194.
45. Baker, R.G.; Hayden, M.S.; Ghosh, S. NF-κB, inflammation and metabolic disease. *Cell Metab.* **2011**, *13*, 11–22.

46. Ni, H.; Zhao, W.; Kong, X.; Li, H.; Ouyang, J. NF-Kappa B Modulation Is Involved in Celastrol Induced Human Multiple Myeloma Cell Apoptosis. *PLoS ONE* **2014**, *9*, e95846.
47. Zheng, L.; Fu, Y.; Zhuang, L.; Gai, R.; Ma, J.; Lou, J.; Zhu, H.; He, Q.; Yang, B. Simultaneous NF-κB inhibition and E-cadherin upregulation mediate mutually synergistic anticancer activity of celastrol and SAHA *in vitro* and *in vivo*. *Int. J. Cancer* **2014**, *135*, 1721–1732.
48. Youn, G.S.; Kwon, D.J.; Ju, S.M.; Rhim, H.; Bae, Y.S.; Choi, S.Y.; Park, J. Celastrol ameliorates HIV-1 Tat-induced inflammatory responses via NF-kappaB and AP-1 inhibition and heme oxygenase-1 induction in astrocytes. *Toxicol. Appl. Pharmacol.* **2014**, *280*, 42–52.
49. Chiang, K.C.; Tsui, K.H.; Chung, L.C.; Yeh, C.N.; Chen, W.T.; Chang, P.L.; Juang, H.H. Celastrol Blocks Interleukin-6 Gene Expression via Downregulation of NF-κB in Prostate Carcinoma Cells. *PLoS ONE* **2014**, *9*, e93151.
50. Yuzefovych, L.; Wilson, G.; Rachek, L. Different effects of oleate *vs.* palmitate on mitochondrial function, apoptosis, and insulin signaling in L6 skeletal muscle cells: Role of oxidative stress. *Am. J. Physiol. Endocrinol. Metab.* **2010**, *299*, E1096–E1105.
51. Houstis, N.; Rosen, E.D.; Lander, E.S. Reactive oxygen species have a causal role in multiple forms of insulin resistance. *Nature* **2006**, *440*, 944–948.
52. Hoffmann, A.; Levchenko, A.; Scott, M.L.; Baltimore, D. The IκB-NF-κB Signaling Module: Temporal Control and Selective Gene Activation. *Science* **2002**, *298*, 1241–1245.
53. Hoffmann, A.; Baltimore, D. Circuitry of nuclear factor κB signaling. *Immunol. Rev.* **2006**, *210*, 171–186.
54. Plomgaard, P.; Bouzakri, K.; Krogh-Madsen, R.; Mittendorfer, B.; Zierath, J.R.; Pedersen, B.K. Tumor Necrosis Factor-α Induces Skeletal Muscle Insulin Resistance in Healthy Human Subjects via Inhibition of Akt Substrate 160 Phosphorylation. *Diabetes* **2005**, *54*, 2939–2945.
55. Werner, E.D.; Lee, J.; Hansen, L.; Yuan, M.; Shoelson, S.E. Insulin Resistance Due to Phosphorylation of Insulin Receptor Substrate-1 at Serine 302. *J. Biol. Chem.* **2004**, *279*, 35298–35305.
56. Aguirre, V.; Werner, E.D.; Giraud, J.; Lee, Y.H.; Shoelson, S.E.; White, M.F. Phosphorylation of Ser307 in Insulin Receptor Substrate-1 Blocks Interactions with the Insulin Receptor and Inhibits Insulin Action . *J. Biol. Chem.* **2002**, *277*, 1531–1537.
57. Hirosumi, J.; Tuncman, G.; Chang, L.; Gorgun, C.Z.; Uysal, K.T.; Maeda, K.; Karin, M.; Hotamisligil, G.S. A central role for JNK in obesity and insulin resistance. *Nature* **2002**, *420*, 333–336.
58. Barja, G. Mitochondrial Oxygen Radical Generation and Leak: Sites of Production in States 4 and 3, Organ Specificity, and Relation to Aging and Longevity. *J. Bioenerg. Biomembr.* **1999**, *31*, 347–366.
59. Nilsson, E.C.; Long, Y.C.; Martinsson, S.; Glund, S.; Garcia-Roves, P.; Svensson, L.T.; Andersson, L.; Zierath, J.R.; Mahlapuu, M. Opposite Transcriptional Regulation in Skeletal Muscle of AMP-activated Protein Kinase γ3 R225Q Transgenic Versus Knock-out Mice. *J. Biol. Chem.* **2006**, *281*, 7244–7252.
60. Kahn, N.Y.; Accili, C.R.; Domenico; Kitamura, A. Mouse Models of Insulin Resistance. *Physiol. Rev.* **2004**, *84*, 623–647.
61. Ciaraldi, T.P.; Mudaliar, S.; Barzin, A.; Macievic, J.A.; Edelman, S.V.; Park, K.S.; Henry, R.R. Skeletal Muscle GLUT1 Transporter Protein Expression and Basal Leg Glucose Uptake Are Reduced in Type 2 Diabetes. *J. Clin. Endocrinol. Metab.* **2005**, *90*, 352–358.

62. Gaster, M.; Staehr, P.; Beck-Nielsen, H.; Schrøder, H.D.; Handberg, A. GLUT4 Is Reduced in Slow Muscle Fibers of Type 2 Diabetic Patients: Is Insulin Resistance in Type 2 Diabetes a Slow, Type 1 Fiber Disease? *Diabetes* **2001**, *50*, 1324–1329.
63. Silva, J.L.T.; Giannocco, G.; Furuya, D.T.; Lima, G.A.; Moraes, P.A.C.; Nachef, S.; Bordin, S.; Britto, L.R.G.; Nunes, M.T.; Machado, U.F. NF-κB, MEF2A, MEF2D and HIF1-a involvement on insulin- and contraction-induced regulation of GLUT4 gene expression in soleus muscle. *Mol. Cell. Endocrinol.* **2005**, *240*, 82–93.
64. O'Neill, H.M. AMPK and Exercise: Glucose Uptake and Insulin Sensitivity. *Diabetes Metab. J.* **2013**, *37*, 1–21.
65. Fujii, N.; Jessen, N.; Goodyear, L.J. AMP-activated protein kinase and the regulation of glucose transport. *Am. J. Physiol.—Endocrinol. Metab.* **2006**, *291*, E867–E877.
66. Lihn, A.S.; Pedersen, S.B.; Lund, S.; Richelsen, B. The anti-diabetic AMPK activator AICAR reduces IL-6 and IL-8 in human adipose tissue and skeletal muscle cells. *Mol. Cell. Endocrinol.* **2008**, *292*, 36–41.
67. Green, C.J.; Pedersen, M.; Pedersen, B.K.; Scheele, C. Elevated NF-κB Activation Is Conserved in Human Myocytes Cultured From Obese Type 2 Diabetic Patients and Attenuated by AMP-Activated Protein Kinase. *Diabetes* **2011**, *60*, 2810–2819.
68. Barma, P.; Bhattacharya, S.; Bhattacharya, A.; Kundu, R.; Dasgupta, S.; Biswas, A.; Bhattacharya, S.; Roy, S.S.; Bhattacharya, S. Lipid induced overexpression of NF-κB in skeletal muscle cells is linked to insulin resistance. *Biochim. Biophys. Acta—Mol. Basis Dis.* **2009**, *1792*, 190–200.
69. Yang, H.; Chen, D.; Cui, Q.C.; Yuan, X.; Dou, Q.P. Celastrol, a Triterpene Extracted from the Chinese "Thunder of God Vine," Is a Potent Proteasome Inhibitor and Suppresses Human Prostate Cancer Growth in Nude Mice. *Cancer Res.* **2006**, *66,* 4758–4765.
70. Im, A.R.; Kim, Y.H.; Uddin, M.R.; Chae, S.W.; Lee, H.W.; Jung, W.S.; Kim, Y.H.; Kang, B.J.; Kim, Y.S.; Lee, M.Y. Protection from antimycin A-induced mitochondrial dysfunction by Nelumbo nucifera seed extracts. *Environ. Toxicol. Pharmacol.* **2013**, *36*, 19–29.
71. Tamrakar, A.K.; Jaiswal, N.; Yadav, P.P.; Maurya, R.; Srivastava, A.K. Pongamol from Pongamia pinnata stimulates glucose uptake by increasing surface GLUT4 level in skeletal muscle cells. *Mol. Cell. Endocrinol.* **2011**, *339*, 98–104.

*Sample Availability*: Samples of the celastrol is available from the authors.